Sampling Error in a Single-instument Vertical Gradient Measurement in the Atmospheric Surface Layer

By
Brian Lincoln Woodruff

Department of Atmospheric Science
Colorado State University
Fort Collins, Colorado

Colorado State University

Department of Atmospheric Science

Paper No. 399

SAMPLING ERROR IN A SINGLE-INSTRUMENT VERTICAL GRADIENT MEASUREMENT IN THE ATMOSPHERIC SURFACE LAYER

by

Brian Lincoln Woodruff

Research supported by the
National Science Foundation
under Grants ATM 8114575
and ATM 8312615.

Department of Atmospheric Science
Colorado State University
Fort Collins, Colorado

April, 1986

Atmospheric Science Paper No. 399

ABSTRACT

The problem of accurately measuring the small vertical gradient of an atmospheric scalar stands against a growing number of dry deposition studies employing profile methods. To resolve a concentration difference of ~1% through the usual approach, subtracting two independent measurements, dictates an instrument accuracy requirement that is prohibitive under field conditions. Another approach, using a single instrument and sampling alternately at two levels, relaxes the accuracy requirement but also introduces sampling errors that are obscure and often neglected. This paper quantifies the sampling error of a one-instrument strategy to measure a scalar vertical difference within the surface layer.

Two sources contribute to sampling error. The first arises from practical limitations on averaging time and is present regardless of ones approach to difference measurement. The second arises when half the available difference information is discarded in an intermittent sampling approach. Each error source depends on the ratio of a time scale of the scalar in turbulent flow and a time scale of the measurement procedure. We derive generalized, dimensionless time scales of a scalar and a scalar difference from scalar variance spectra in an unstable surface layer.

One-instrument sampling error is found through simulation: starting with continuous temperature time series obtained at two levels, we form an intermittent data record by "sampling" alternately from the lower and upper time series and then compare the temperature difference computed from intermittent and continuous data records. Sampling error increases monotonically with the length of the down and up cycle; good experimental design will therefore employ the shortest practicable cycle time. The lower limit of cycle time is controlled by the measurement time wasted at each height transition (dead time), including instrument response time and the operating time of, eg., an elevator or an alternating sampling valve. Sampling error may be estimated for any scalar difference measurement in an unstable surface layer, given averaging time, intermittent-cycle time, deadtime, wind speed, and measurement heights.

ACKNOWLEDGEMENTS

This material is based upon work supported by the National Science Foundation under Grants No. ATM 8114575 and ATM 8312615. Research facilities at the Boulder Atmospheric Observatory were provided by the National Oceanic and Atmospheric Administration. Computing resources were provided by the Scientific Computing Division of the National Center for Atmospheric Research. The National Center for Atmospheric Research is sponsored by the National Science Foundation.

DEDICATION

This thesis is dedicated to the late Frank Melchior, who designed electronics for the the "down and upper," and to Froda Robin Greenberg, who vowed never to type my masters thesis, and she didn't.

TABLE OF CONTENTS

APPENDICES (continued)

LIST OF FIGURES

LIST OF SYMBOLS

c_p	specific heat of air at constant pressure
coh	coherence
D	sample inlet diameter
E_i	forcing function (instrument input, eg. gas concentration)
E_o	response function (instrument output)
E_1	constant value of forcing function following height transition
f	frequency
f_N	Nyquist frequency or folding frequency
F	flux
K	eddy diffusivity
L	Obukhov length
n	dimensionless frequency
N	number of cases
P	power spectrum
r	correlation coefficient
R_e	Reynolds number
s	arbitrary scalar variable
<S>	ensemble mean of s
t_a	averaging time or run length
t_e	elevator transit time
t_I	cycle time ("down and up" cycle)

t_r	instrument response time (e-folding time)
t_0	blanking time at height transition ("dead time")
T	temperature
ΔT_C	temperature difference (computed from continuous data)
ΔT_I	temperature difference (computed from intermittent data)
u	horizontal wind component
V	sample inlet velocity
w	vertical wind component
z	height above surface
γ_d	dry adiabatic lapse rate (0.0098 K m^{-1})
ε	combined sampling error of intermittent gradient measurement (estimate)
ε_a	standard error of means computed over averaging time t_a, relative to the ensemble mean
ε_I	mean deviation of ΔT_I about ΔT_C
θ	potential temperature
$\Delta\theta$	potential temperature change, taken as $\Delta\theta = \Delta T + \gamma_d \Delta z$ in the surface layer
μ	air viscosity
ρ	air density
σ	standard deviation
τ	time scale (f_{max}^{-1} at peak of variance spectrum)
τ_*	dimensionless time scale
T	integral time scale

1. INTRODUCTION AND SUMMARY

The investigator who wants to measure the vertical gradient of an atmospheric scalar confronts a classic experimental problem: measuring the difference of two values. A scalar such as temperature, humidity, or chemical concentration can exhibit a very small vertical gradient, and the difficulty lies in making an accurate measurement of the attendant small vertical difference. The obvious method is to take measurements at two levels with two instruments and subtract the results, but unless the instruments used are extremely precise, the measurement errors may exceed the small differences being measured. Furthermore, any mismatch in the calibration or the drift of the instruments relative to each other will contribute to errors in the difference measurement.

Both these error sources may be avoided if the difference is measured with a single instrument that samples alternately at two levels. In the measurement of gas concentrations, for example, this can be arranged either by raising and lowering the sample inlet at predetermined intervals or by using fixed inlet lines at two levels and a valve that samples from each line alternately. The vertical difference is computed from successive measurements made with a single instrument, and the investigator is pleased to avoid the operational and error problems of dual instrumentation. However, he or she obtains these advantages at a price: since the single instrument can sample at only one level at a time, the technique necessarily disregards half of the information

available to determine the gradient and therefore introduces a new source of error into the measurement. This is a kind of sampling error because it results from the strategy of estimating a mean value from an incomplete sample of the available information. The single-instrument approach thus trades one set of error sources for another source which is less well understood and may be severe.

Among his suggestions on vertical profile measurements, Kaimal [1975] placed a warning: "It is important that the measurements be made simultaneously by individual instruments at each height, never by sampling at different heights in turn, as this would introduce serious sampling errors." The aim of this paper is to quantify the sampling error of the intermittent sampling technique so that the investigator who chooses to disregard Kaimal's admonition may appreciate the error penalty involved and reduce that penalty through experiment design.

Previous One-Instrument Gradient Measurements

An important application of vertical gradient measurements is the determination of surface flux for various trace gases, also referred to as dry deposition. There are several methods for making flux determinations from vertical gradients (called profile-flux methods), all based on the concept that the vertical flux is proportional to the vertical gradient of the gas and in the opposite direction from the gradient. This concept is called K-theory, after the proportionality constant, K, also called the eddy diffusivity. In practice, profile-flux determinations require an independent measurement of the diffusivity, which is then multiplied by a measured vertical gradient to arrive at the flux. More and more such flux determinations are being made as atmospheric chemists become interested in studying the dry

deposition rates of tropospheric trace gases, and as new instruments are developed for that purpose. Any such instrument must be able to resolve a vertical difference of about 1% in concentration over a two-fold height interval according to Hicks et al. [1980]. In the world of practical instrumentation such a requirement is prohibitive. These authors even suggest the use of a single instrument measuring at several heights to eliminate the systematic differences among sensors, but they do not discuss the sampling errors that are introduced by this scheme.

Several researchers have resorted to the single-instrument method for a gradient measurement, yet none have fully explored the attendant sampling errors. For example, Willis and Paulson [1963] noted sampling error during the development of a sampling system they called the roving probe, whose purpose was to measure vertical profiles over water surfaces. The roving probe consisted of temperature and wind speed sensors mounted on a movable carriage which travelled among six logarithmically-spaced sampling heights (transit time approximately 1 s, sampling time at each level approximately 10 s). The sensors were on station at each sampling height intermittently for a total of roughly 1/6 of each run, and the average sensor output at each level was used to form the mean profile. Willis and Paulson found that the greatest source of error in this sampling scheme was the sampling error introduced by disregarding 5/6 of the available data at each level. They further showed that the sampling error increased as the total probe cycle time increased, a result which turns out to be of crucial significance to the present work. They decided to reduce the sampling errors of the roving probe by adding a second sensor which measured continuously at a fixed height. At the height of the continuous sensor,

the means of the continuous and intermittent data were calculated, and their ratio was used as a correction factor for all six levels. Thus the roving probe technique, though successful, still required the addition of a second instrument to reduce sampling error.

In another experiment using a single instrument to measure a concentration difference, Delany and Davies [1983] reported measurements of trace gas dry deposition by the profile-flux method. They used a single sampling line, the intake of which was positioned alternately at 0.125 m and 1.75 m for 60-s intervals by a motor-driven pulley system (transit time 10 s). The mean vertical gradient for a run was found by averaging over the values at each height separately, then taking the difference (data taken during the 10 s transition periods were disregarded). Although the dry deposition values reported by Delany and Davies were in the range previously reported in the literature, their discussion of experimental error did not include the sampling error of their gradient-measurement scheme.

In a field comparison of dry deposition measurement methods [Dolske and Gatz, 1985] the profile-flux method was used by Davis and Wright [1985], who wanted to demonstrate that dry deposition of sulfur dioxide could be measured with a single, sensitivity-enhanced sulfur dioxide analyzer. Their sampling method used fixed intake lines positioned at four heights on a tower, with a valve to switch the gas analyzer among the four lines. At each height, 20-s measurements were made 22 times over a run of 1.8 ks (30 min), and the vertical gradient of concentration was calculated by linear regression of concentration against the logarithm of height. Davis and Wright estimated that the uncertainty in their calculated deposition velocities ranged up to 600% and decided

to forego further analysis in the face of such high error rates. They attributed the uncertainty to the very low mean concentration ($3.3\ \mu g\ m^{-3}$), which severely tested the capabilities of their instrument, and speculated that changing surface and atmospheric conditions might be an additional error source. The possible introduction of sampling errors by the intermittent nature of their sampling scheme was not discussed.

A final example of a profile-flux measurement using an intermittent gradient sampling scheme is provided by the Surface Layer Atmospheric Chemistry Experiment (SLACE), which was carried out in 1983. SLACE had several objectives which are described in Appendix A; one of these was to compare the profile-flux method with the eddy-correlation method, the benchmark for determining the flux of a trace gas. In the eddy-correlation method, vertical velocity and gas concentration are measured with high time resolution, and gas flux is calculated as their covariance (covariance is the time-average product of perturbations of two variables about their respective means). Eddy correlation is considered the most rigorous experimental method to determine the flux because it does not require any assumptions about the statistics of the turbulent flow in which the measurement is made; rather, eddy correlation samples the turbulent eddies directly. However, the chief drawback is that instruments used for eddy correlation must be fast enough to respond to the smallest eddies that contribute to the flux; the bandwidth required is $3\bar{u}/z$ [Kaimal, 1975], typically about 10 Hz in the surface layer. The instrumentation demands of the eddy-correlation method motivate the current active development of profile-flux methods and, hence, techniques to measure the vertical gradient of scalars.

In the SLACE comparison study the flux of ozone was simultaneously determined by the eddy-correlation and profile methods. The profile-flux method used is called the Modified Bowen-Ratio [Hicks and Wesely, 1978],

$$F_{O_3} = \overline{w'T'}(\Delta\overline{O_3}/\Delta\overline{\Theta})$$

where F_{O_3} is the flux of ozone (units: ppb m s^{-1}), w and T are vertical velocity and temperature, primes denote perturbations about the mean, and overbars represent time averages. In this method the scalar diffusivity is given by the ratio of the heat flux $\overline{w'T'}$ (measured by eddy correlation) to the gradient of mean potential temperature $\Delta\overline{\Theta}$. The gradient of ozone was obtained with a single ozone analyzer by raising and lowering the inlet of its sampling line so that a concentration was obtained at two levels alternately. A device fabricated for this purpose could be programmed to move the sample inlet between selected levels and wait for a selected sampling period at each level. This device, which came to be known as the "down and upper," was set to operate between 1 m and 6 m, changing position every 180 s (3 min) for a total cycle time of 360 s (6 min), with a transit time between levels of 18 s. Mean gradients were calculated as in Delany and Davies [1983], by averaging the up periods and down periods separately, then taking the difference. Details of the field experiment and data analysis can be found in Appendix A.

Figure 1 shows the result of the comparison of 1.2-ks (20-min) mean ozone flux for one morning of the SLACE field study. There is only a rough correspondence between the two time series ($r = 0.3$); the gradient method results are much more variable than the eddy correlation results and also tend to underestimate the downward ozone flux. Yet the

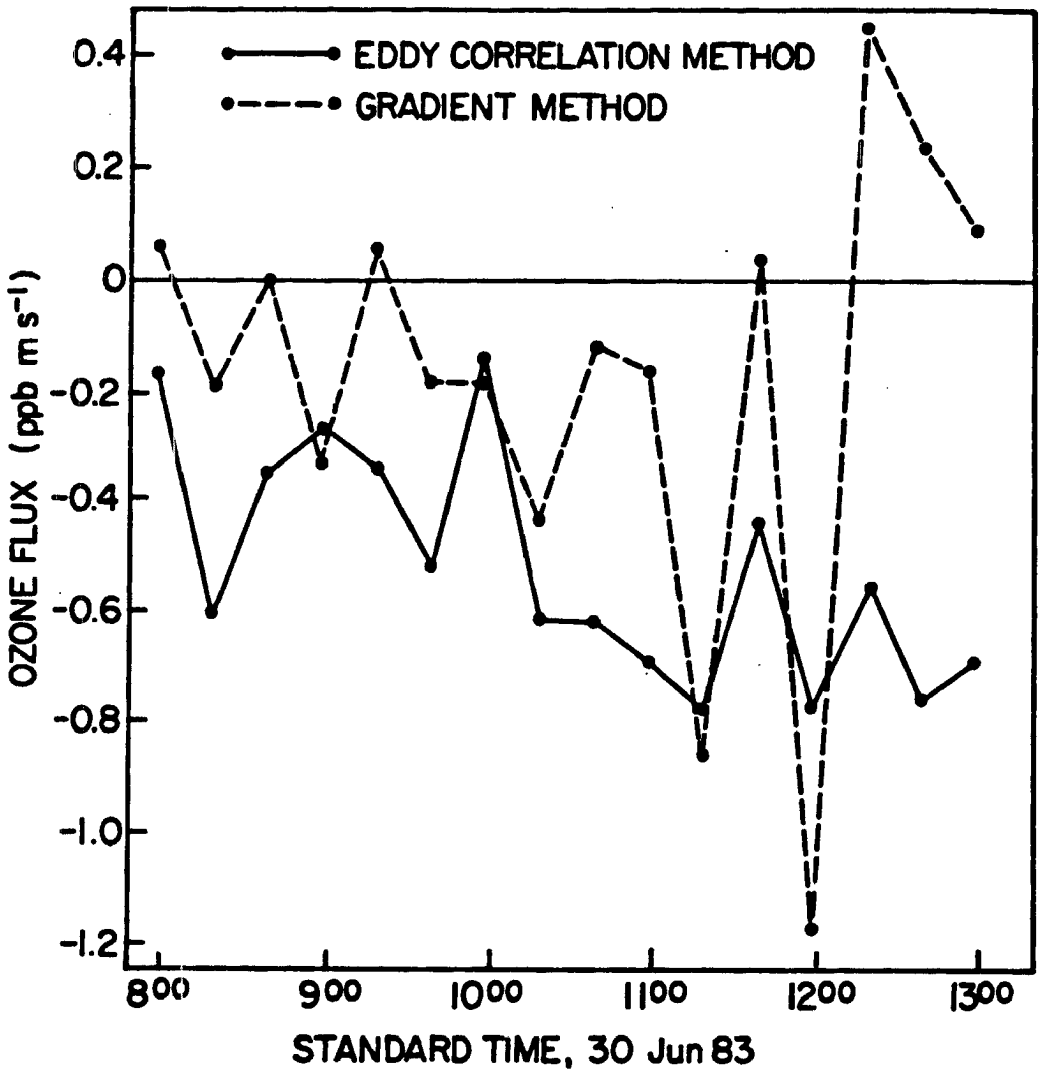

Figure 1. Comparison of 1.2-ks (20-minute) mean ozone flux measurements. Flux by eddy correlation is downward (negative), consistent with ozone destruction at the surface. Flux by the gradient method is sometimes upward, suggesting that the ozone gradient measurement (concentration decreasing upward) is not accurate.

most disturbing result of the gradient method is that the flux sometimes goes positive (upward), which, if correct, calls into question a well-known property of ozone: its reactivity as an oxidant. Because ozone is rapidly consumed on contact with the surface, its flux is constrained to be either negative (downward) or zero. A check on the signs of terms in the Bowen ratio equation shows $\overline{w'T'}$ positive and $\Delta\bar{\theta}$ negative throughout the morning, as expected, but during the anomalous periods the measured ozone gradient is negative (decreasing upward), suggesting a surface source, rather than sink, for ozone. Thus the gradient measurement method proves unable to correctly resolve even the sign of the ozone gradient and is an important cause of the poor agreement between the two flux measurement methods.

As these four examples indicate, investigators who use a single instrument with an intermittent sampling scheme to measure a vertical gradient have encountered significant uncertainty from a source that is not well understood. Willis and Paulson [1963] determined that source to be sampling error and identified probe cycle time as a controlling variable, but they did not attempt to quantify the sampling error. The present work quantifies the sampling error involved in making a gradient measurement with a single instrument and relates that error to the intermittent sampling scheme used in the measurement. The results should be applicable in the design of gradient sampling schemes to be used in the dry deposition studies that are becoming increasingly common today.

The Role of Averaging Time

Before approaching the problem of error due to intermittent sampling we must recognize that another form of sampling error is present in the gradient no matter how it is measured, even if we use an inherently differential measuring device. This error arises from the practical requirement that measurements of a mean quantity in a turbulent flow must be made over a finite averaging time. Each measurement period constitutes only one realization of the turbulent flow that occurs under the current atmospheric conditions. If measurements were made over several periods with similar wind speed and temperature profiles, then the means would vary about a value called the ensemble mean, which is the value we would obtain if we averaged a large number of realizations of the flow. The time averages from our experiment will approach the ensemble mean as the averaging time increases, as long as the atmospheric and surface conditions which regulate the turbulent flow do not change (such a turbulent flow is called "stationary"). Because the real atmosphere does not provide constant conditions, there is a practical limit to averaging time, and the time averages we compute will deviate from the ensemble mean. This is the basic sampling error present in the gradient measurements; errors attributable to intermittent sampling are additional.

The averaging-time sampling error is treated in Chapter 2 using an analytical approach based on the relationship of averaging time to the time scale of the measured variable. The time scale is a measure of the time lag over which a time series is correlated with itself (autocorrelated); it may be interpreted as the time required for a dominant-sized eddy to pass a fixed point, e.g., a sensor mounted on a tower.

One conclusion drawn from the investigation of time scales is that the time scale of a difference measurement is significantly shorter than the time scale of a measurement at one level. This suggests for a given error level the averaging time required to make a gradient measurement is shorter than it is for an absolute measurement at a single level, so that averaging time requirements may be relaxed somewhat for gradient measurements.

The Role of Cycle Time

We turn now to the error contributed by intermittent sampling. These errors were determined empirically, beginning with a set of high-quality temperature gradient observations taken with fast-response continuous instrumentation at two levels. Various single-instrument measurements were simulated by "sampling" alternately from these two time series, and the error attributable to the intermittent sampling scheme was then found by comparing the resulting gradient with that computed using the full continuous data record. In other words, the two continuous instruments are assumed for this purpose to give the "true" temperature gradient, and we ask How well does intermittent sampling reproduce the gradient result from continuous sampling? This procedure was applied to forty-two 1.8-ks (30-min) periods with unstable lapse rates to obtain statistics on the behavior of the sampling error. The length of the "down and up" sampling cycle was varied in the simulations to determine the sensitivity of the sampling error to this variable. Another variable similarly tested was the amount of "dead time": this is the amount of data that must be disregarded at each height transition, which includes transit time between levels and time required for instrument output to approach a stable value at the new level.

The most significant finding of the simulations is that the sampling error increases rapidly with probe cycle time; Figure 2 illustrates the result for zero dead time (i.e., transit time and instrument response both instantaneous). The ordinate is the mean deviation of the "intermittent" gradient about the "continuous" gradient for the 42 cases, in percent. The abscissa gives the probe cycle time t_I normalized by the time scale τ of the upper temperature time series, defined in Chapter 2. The sampling error is seen to increase linearly on this log-log plot, indicating that the error increases as the 0.8 power of t_I/τ. In further simulations, the dead time was allowed to take on values greater than zero, but the resulting error rate was essentially the same in the range 0 to 0.2 of the probe cycle time. Provided that the dead time is small compared to τ, the dead time is much less significant than the probe cycle time in determining the sampling error of an intermittent sampling scheme.

It will be evident that to minimize sampling error, probe cycle time must be held to a fraction of a time scale, the shorter the better. That the temperature time series has a time scale at all suggests the nature of the sampling error of an intermittent gradient measurement. Suppose two time series fluctuated about their means in a truly random way (as in white noise); then there would be no autocorrelation in the time series for any lag time and their time scales would be zero. Sampling intermittently between two such time series to obtain a mean difference would involve some sampling error since half the information is then lost, but that error would be independent of the probe cycle time used. However the time series are, in fact, autocorrelated (and therefore possess time scales) because of the structure imposed by

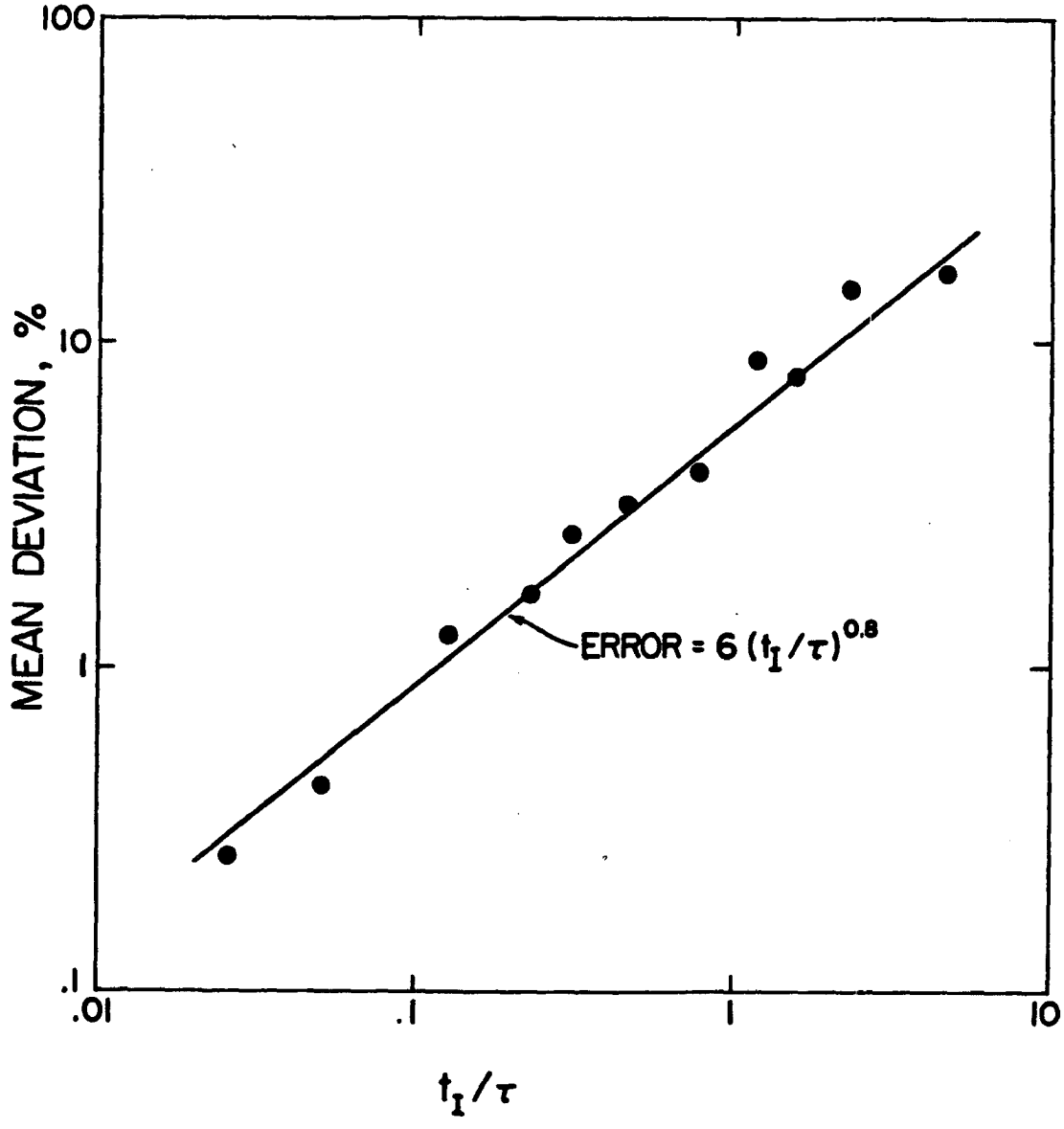

Figure 2. Relative sampling error in an intermittent gradient measurement (zero-dead-time case). Error is calculated as the mean deviation

$$\text{ERROR} = (100/N) \sum |(\Delta T_I - \Delta T_C)/\Delta T_C|$$

of 42 cases with unstable lapse rates, where subscripts I and C indicate that the gradient is computed from intermittent and continuous data, respectively. The abscissa is probe cycle time normalized by the temperature time scale τ (the time scale is defined in Chapter 2: it is the inverse frequency at the maximum of the scalar variance spectrum).

eddies as they pass the sensor. Given an unstable lapse rate, for example, we may visualize a typical eddy whoose leading side brings down cooler air from aloft, while its trailing side brings up warmer air from below. When we add to this picture a gradient-measuring scheme which samples alternately at two levels in the eddy as it passes by, it is not surprising that the measured gradients depend on the relationship between the time scale of the eddies and the time scale of the intermittent sampling procedure.

The results shown in Figure 2 apply not only to temperature measurements but to any other scalar as well: one need only estimate the time scale of the scalar to estimate the sampling error for a given probe cycle time. One may ask, Are we justified in assuming that temperature behaves like other scalars for the purpose of studying the sampling error of a gradient measurement? We have seen that the sampling error depends on the ratio of the probe cycle time to the temperature time scale, so the use of temperature as a surrogate for the other scalars may be justified if the time scale of temperature is representative of other scalars. In practice the time scale is derived from the variance spectrum of a time series, either by integrating the autocorrelation function (the Fourier transform of the spectrum) or, more simply, by inverting the frequency of the spectral maximum; therefore we need only determine whether the spectra of temperature and other scalars behave alike. Panofsky and Dutton [1984] point out that the spectra of scalars obey Monin-Obukhov scaling in the surface layer: the normalized spectrum of any scalar is a dimensionless function only of frequency and the dimensionless stability parameter z/L, where z is measurement height and L is the Obukhov length. They further observe

that, while in principle the spectra may be different for different scalars, to date no significant differences have been confirmed; they therefore assume that the dimensionless spectrum of temperature applies to all scalars. Thus, for the limited purpose of this study, we have reasonable justification for asserting that the results obtained with temperature data apply to other scalars as well.

Recommendations

The information developed in this study may be used in the design of field experiments where vertical gradients are to be measured. The investigator who has an instrument capable of making the differential measurement directly is indeed fortunate, as he or she need not consider sampling errors other than those contributed by averaging time considerations. However, in the normal situation where instruments can monitor only one level at a time, choices must be made which affect the errors present in the results, choices based on availability of equipment. If only one instrument is available, then an intermittent sampling scheme is the only recourse: in the case of gas measurements, the investigator may use either a single inlet line with a device to move it between levels or two inlet lines with a valve that switches the instrument alternately between lines. (When using multiple inlet lines, care must be taken to assure identical conditioning of the lines lest they induce differential effects on the sample air and thus add to the uncertainty of the gradient measurement.) The most important design criterion for such a system is that the cycle time of the intermittent sampling be minimized. The sampling error for any given combination of cycle time, transit time, and instrument response time may be estimated using the

diagrams presented in Chapter 3. Although the results presented here apply to two-level gradient measurements, it is likely that systems that sample at more than two levels [eg., Dolske and Gatz, 1985] can also reduce sampling error by reducing cycle time.

When two instruments are available, the investigator may use both of them at fixed levels, with the attendant systematic error of differencing the output of two instruments, or may use only one instrument and incur the error penalty of intermittent sampling. The information presented in Chapter 3 makes possible an informed choice between these two alternatives. However, as long as the hardware needed for intermittent sampling is ready to hand, there exists a third alternative: to use both instruments and arrange them to sample alternately at each level by periodically exchanging positions. The gradient is then computed as the average of the gradient results of each independent instrument. This is the approach used by Droppo [1985] with good results. It can be shown analytically that the result is equivalent to a system using two fixed instruments with all systematic error removed, as long as calibration of each instrument remains constant over a run. Some data are lost during the exchange of levels (dead time), but we have seen that the dead time, if moderate, makes only a minor contribution to sampling error. In any case, the amount of lost data can be minimized by exchanging the positions of the two inlet lines only once during a run, since there is no advantage to switching them more often. Again assuming negligible drift over a run, this approach is nearly as free of sampling error as a single, inherently-differential instrument and should be adopted whenever appropriate equipment is available.

Limitations

The reader should be aware that these results have certain limitations. The sampling error of a single instrument which samples alternately at two levels has been found empirically using temperature data taken at 4 and 8 meters. A general consideration guides the selection of sampling heights in a one-instrument gradient measurement: to maximize the gradient. This can be done by increasing the height interval and/or by choosing the lower height as small as possible. The lower limit is about 100 times the surface roughness length [Garratt, 1980] to avoid wake effects from the roughness elements. Note also that the results are limited to daytime conditions with unstable lapse rates; extension of this research to neutral and stable lapse rates (overcast and nighttime conditions) may reveal that the sampling error depends on the stability regime. Although two contributions to sampling error are discussed in this study (limited averaging time and intermittent sampling), the combination of these to produce a total resultant sampling error is treated using the conservative assumption that they are additive. Further research may prove that the two error sources are independent and random and thus lead to a more realistic (smaller) total sampling error. A final caveat regards the use of continuous instrumentation in this study. The results do not apply to an instrument of the sample-and-hold variety, such as the Dasibi Ozone Monitor, Model 1008-AH (Dasibi Environmental Corp., 616 E. Colorado, Glendale, CA 91205), which introduces additional sampling error because it disregards a good deal of available data during the hold phase of its sampling cycle. The latter sampling error can be characterized using simulation techniques like those presented here and is left for a future investigation.

The remainder of this thesis gives a more detailed development of the ideas presented above. The next chapter describes the sampling error involved in making any measurement of a mean quantity in a turbulent flow with a limited averaging time. Chapter 3 extends the discussion to consider the additional error introduced by sampling a gradient intermittently with a single instrument, including the contributions of probe cycle time, probe transit time, and instrument response time. Appendices include an overview of the SLACE field study and data processing, a description of the temperature gradient data set used to derive scalar timescales and the intermittent sampling error, and the derivation of a recommended dead-time formula.

2. GRADIENT ERROR WITH TWO SENSORS

The discussion of sampling error in measuring a vertical gradient must begin with that form of error attributable to the limited sampling time available for a real measurement in the atmospheric surface layer. We begin with a brief catalog of the possible sources of error in making a vertical gradient measurement, mostly to distinguish which error sources are dealt with here and which are not. An analytical expression is next presented that estimates the error contributed by a finite averaging time. The remainder of the chapter introduces the set of temperature gradient data that are used as a surrogate for all scalar variables in the surface layer and presents time scales derived from the temperature dataset which are then used to estimate averaging-time error.

There are several possible sources of error in making a vertical gradient measurement in the surface layer, only one of which will be discussed in this study. One error source category is simply the failure of assumptions underlying the calculation method. We seek time-average values of scalar quantities, but for the time averages to be meaningful requires that the turbulent flow time series from which the averages are derived is stationary in both space (horizontal homogeneity) and time. Error due to non-stationarity is presumed negligible for the purpose of this study.

The second error category includes instrumental and data acquisition sources. Instrument accuracy, ie., calibration and drift, are of primary importance when measuring vertical differences on the order of 1% with multiple instruments; the difficulty of maintaining intercalibration motivates the development of schemes to do the measurement with a single instrument. In this error category we must include the calibration of any signal processing devices preceeding the data acquisition system, eg., the voltage offset circuits used in SLACE to match the voltage range of the signal to the voltage range of the data acquisition system. And finally there is the variance imposed on the recorded data by the digitization process, amounting to one count of the analog-to-digital converter. None of the error sources in this category are considered in this study.

The last error category, and the principal focus of this work, is sampling error. Here we are concerned with error introduced as a consequence of our strategy for extracting mean vertical gradients from a turbulent flow. Two aspects of sampling error are discussed in this and the following chapter. The first is error introduced by our selection of a finite averaging time, an error source that is always present regardless of our choice of instruments. The second is error introduced by sampling intermittently with a single instrument. (A third form of sampling error is introduced if the instrument used does not monitor continuously, but is rather of the sample-and hold type. Such an instrument disregards considerable data during the hold phase of its cycle. However this source of error is not dealt with here, as the data used in this report were taken with continuous instruments.) In Chapter 3 we shall assume that these two errors are additive, but this

is a conservative assumption: since both kinds of sampling error arise from stochastic processes which may be independent, we would expect the total relative error to be less than the sum.

The Averaging Time Equation

In a real experiment the period of averaging must be selected with two factors in mind. It must be long in relation to the turbulent fluctuations so that a stable average is achieved. Yet it must be short relative to diurnal variations, since conditions are required to be at least quasi-stationary during the averaging period. In practice Hicks and Wesely [1978] suggest averaging longer than 0.9 ks (15 min) and shorter than 3.6 ks (1 hr). Our choice is based on practical constraints, but the sampling error of our measurement depends on this choice.

Each sensing device measures a quantity s over an averaging time t_a, giving a local mean value $\bar{s}$. But due to the stochastic nature of turbulent flow, each time period t_a must be considered as only one realization of the flow under the given conditions of wind speed, vertical wind shear, temperature lapse rate, and surface roughness. Additional measurements made under similar conditions will produce varying results. The quantity we desire is the ensemble mean $\langle s \rangle$, the mean we would obtain were we to average many measurements made under similar conditions. The ensemble mean would also be obtained if we were to make the measurement with a large number of identical sensors spaced widely over a uniform surface so that each sensor measures a different realization of the flow. Lumley and Panofsky [1964] presented an expression relating the probable error relative to the ensemble mean of

a single measurement made with a finite averaging time:

$$(\sigma_s/\langle s\rangle)^2 \approx 2(T_s/t_a)[\overline{(s-\langle s\rangle)^2}/\langle s\rangle^2] \qquad (1)$$

Here σ_s^2 is the variance of the means $\bar{s}$ about the ensemble mean $\langle s\rangle$, T_s is the integral time scale of s, and $\overline{(s-\langle s\rangle)^2}$ is the ensemble variance of s about the ensemble mean $\langle s\rangle$. It will come as no surprise to the experimentalist that the dimensionless ratio, variance to mean-squared, appears in this expression. The other dimensionless ratio T/t_a is more interesting: it indicates that for $\bar{s}$ to converge with $\langle s\rangle$ requires the choice of an averaging time large relative to the integral time scale T. As we have seen, practical constraints do not always permit such a choice, but (1) gives an estimate of the error introduced by our choice of averaging time based on measured or estimated properties of the time series s.

This expression may be simplified somewhat for our purposes. Since in practice the ensemble variance and ensemble mean are not known, the sample variance and mean are used to estimate them, thus

$$\overline{(s-\langle s\rangle)^2}/\langle s\rangle^2 \approx \overline{s'^2}/\bar{s}^2 \qquad (2)$$

where $s'=s-\bar{s}$. The term $\overline{s'^2}/\bar{s}^2$ may be estimated prior to making measurements or can be evaluated numerically afterward.

The integral time scale T may also be simplified. It is formally defined as the integral of the autocorrelation function from lag time zero to infinity. In practice, however, the autocorrelation function must be calculated from a finite-length time series so that the autocorrelation function is not known for lag-time values larger than the length of the data record. This and other drawbacks prompted Panofsky and Dutton [1984] to suggest that a different time scale be used to describe atmospheric data. Their method first requires that the power

spectrum be obtained from a time series, eg., by the Fourier transform. The spectrum is then multiplied by frequency and plotted against frequency, as in Figure 3. Values on such a curve are in units of variance per unit log-frequency interval. This type of display is common practice in the description of atmospheric spectra, and one reason for this popularity is that the spectral curve typically has a maximum. Panofsky and Dutton suggest that the inverse of the frequency at the spectral maximum is a useful time scale τ, which is typically four to six times the integral time scale T. This time scale may be interpreted as the time required for a dominant-sized eddy to passed a fixed point, say, a sensor mounted on a tower. Using the approximations $\tau \approx 5T$ and (2) we obtain a simplified expression for the relative error ε_a due to the choice of averaging time t_a,

$$\varepsilon_a^2 = (\sigma_s/\langle s \rangle)^2 \approx (2/5)(\tau/t_a)\overline{s'^2}/\bar{s}^2 \qquad (3)$$

If we let s be the scalar difference ΔT, then this expression may be used to determine the effect of averaging time on a scalar difference measurement. To evaluate (3) we must first find typical values for the time scale, variance, and mean of a scalar difference.

A Temperature Gradient Experiment

The method used in this study to evaluate the terms in the averaging time equation is to derive them from the dataset obtained during the SLACE field study. A brief description of the data is appropriate at this point. This data set is also used in Chapter 3 to determine empirically the error contribution of intermittent sampling.

The only scalar gradient measured using two sensors during SLACE was temperature. Platinum-wire thermometers were positioned at 4 m and 8 m and were sampled at a 10-Hz data rate. These thermometers were part

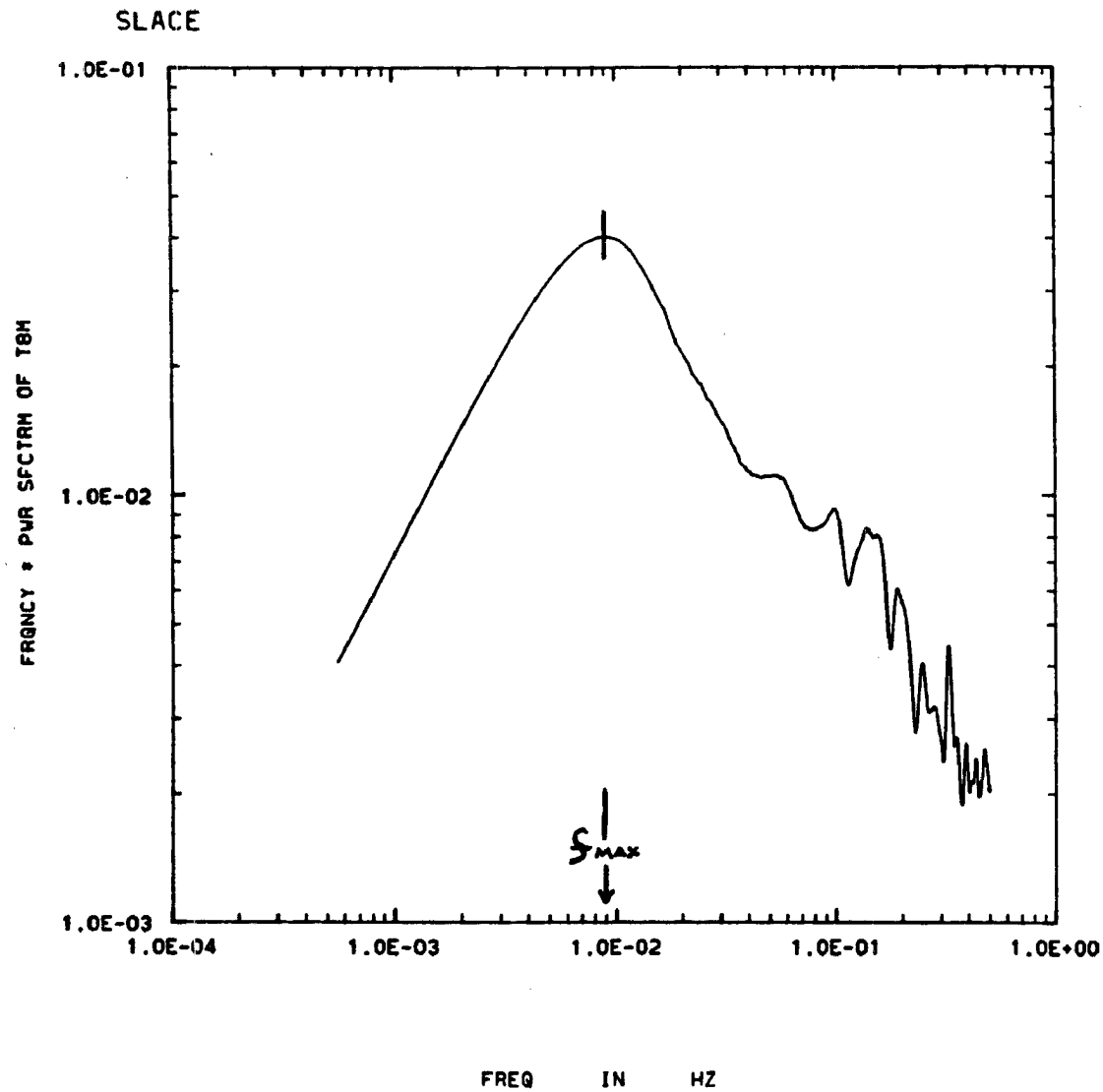

Figure 3. Example variance spectrum. Ordinate is frequency times power spectral density, giving units of variance per unit log-frequency interval. The value $1/f_{max}$ is a useful time scale.

of the instrumentation to determine the flux of heat by the eddy correlation method. A second temperature gradient measurement system with a data rate of 1 Hz was operated at the site, but its data was contaminated by noise signals of unknown origin and was thus rejected. Inspection of the 10-Hz data at 4 m and 8 m showed no evidence of the offending noise signal. Thus the 4 m and 8 m temperature data constitute a set of high-quality and high-resolution observations of a scalar gradient, and they were taken as the basic data for use in this study. Note that any scalar gradient would have served this purpose had data been available. We have seen that sampling error is a function of the ratios of time scales in the measurement and, because the dimensionless spectra of scalars are indistinguishable [Panofsky and Dutton, 1984], the time scales derived from such spectra are the same for all scalars. However, equivalence of spectra may not hold for a scalar that is not conserved, eg., the concentration of a chemically reactive gas.

The 4 m and 8 m data were preprocessed for the purposes of this study: the time series were filtered to a 1 Hz data rate, the diurnal temperature variation was removed, and the two time series were subtracted to produce the gradient (difference) time series. The data record comprised 42 cases of 1.8 ks (30 min), representing unstable (daytime) atmospheric conditions. A subset of the data was divided into 21 periods of 1.2 ks (20 min) for convenience in obtaining spectral distributions. The details of the data processing and atmospheric conditions are found in Appendix B.

Timescale of a Scalar and Scalar Gradient

To evaluate the sampling error of a scalar vertical difference measurement we must know its time scales. The error contribution of averaging time (Eq 3) is a function of the difference time scale τ_Δ; the contribution of cycle time (Eq 10, developed in the next chapter) is a function of the time scale τ at one level. The time scale has been previously defined as the inverse of the frequency at the maximum of a variance spectrum; in this section we therefore examine the spectra of temperature and temperature difference in order to find their time scales. We will see that τ and τ_Δ are functions of stability, wind speed, and measurement height; therefore the time scales we derive from the SLACE data set are applicable only to local conditions. The second objective of this section, then, is to find dimensionless (scaled) timescales τ_* and $\tau_{\Delta*}$ which are applicable to any gradient measurement in the surface layer.

The spectrum of a scalar difference has received no attention in the literature, but the spectrum of a scalar at a single level in the surface layer has been investigated by Kaimal et al. [1972]. Their generalized spectrum for temperature, here reproduced in Figure 4, shows that under stable conditions ($z/L > 0$) the spectra fall into distinct categories of z/L, while the unstable spectra all crowd into the narrow band indicated by the hatched area. Note that Kaimal et al. have used dimensionless frequency $n=fz/\bar{u}$ as the abscissa; the inverse of dimensionless frequency is dimensionless time. We therefore define the dimensionless time scale τ_* as the value of $1/n$ at the peak of the

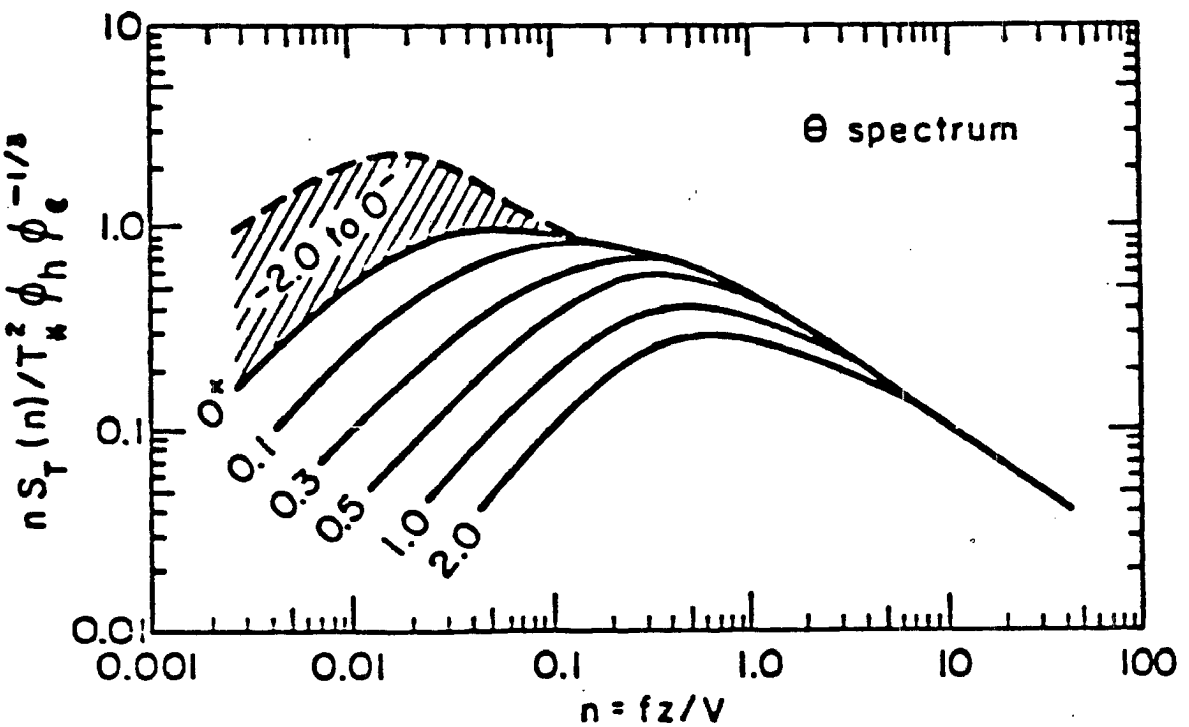

Figure 4. Generalized temperature spectrum for z/L values ranging from +2.0 to -2.0 [source: Kaimal et al., 1972]. Abscissa is dimensionless frequency, ordinate is dimensionless temperature variance.

generalized spectrum, thus

$$\tau_* = 1/n_{max} = \bar{u}/zf_{max} = \tau(\bar{u}/z)$$
$$\tau = \tau_* z/\bar{u} \qquad (4)$$

An estimate of τ_* is at once available for any given stability from the generalized spectrum. For example, as the present study is limited to unstable conditions, we may expect the temperature spectral peak to fall between the peaks of the two curves bounding the hatched area. Inspection of Figure 4 shows that $20<\tau_*<50$ for $-2<z/L<0$. To illustrate the usefulness of this result we may now obtain an estimate of the average time scale of temperature for the subset of temperature data described in Appendix B. Using the 21-case average $\bar{u}=2.5$ m s^{-1} at height $z=8.9$ m places the average temperature time scale for the data subset in the range $70<\tau<200$ seconds. We will check this result using actual spectra from the data subset.

The spectra of temperature and temperature difference were evaluated for 21 periods of 1.2 ks (20 min). The spectra were found using SPECFT, a computer subroutine available at NCAR and based on the fast Fourier transform. Each spectral curve was encouraged to show a distinct and unique maximum by smoothing it with a digital filter (Hamming window of 51 weights); the frequency of the spectral maximum was then found by inspection of the resulting spectral plot. The spectra for 8-m temperature all have distinct maxima with an average $\tau=80$ s, in agreement with the estimate made above using the generalized spectrum of Kaimal et al. The temperature gradient spectra are less well-behaved: while they do have central maxima, these are broad and irregular making it difficult to determine f_{max}.

Because selecting maxima from the irregular ΔT spectra was so subjective, the spectra were further smoothed by forming composite spectra in the hope of obtaining more reliable estimates of the time scales. Prior to compositing, spectral values from each case were normalized by the total variance of the time series for that case, in effect equalizing the areas enclosed by the spectra. The composite spectrum was then obtained by averaging the spectral values by frequency band. (Although not essential to our present purpose, a composite with a more distinct maximum might be achieved if the frequency were also put in the dimensionless form $n=fz/\bar{u}$ prior to compositing; this effort is left for a future investigation.) The resulting composite spectra for T and ΔT are shown in Figure 5. The spectral maximum of ΔT is still rather broad in comparison with the distinct peak of the T spectrum. Yet it is clear that the center of this broad peak is significantly higher in frequency than the peak for T, making the average time scale of ΔT shorter than that for T. By inspection of the composite spectra the time scales are $\tau \approx 80$ s and $\tau_\Delta \approx 20$ s, in agreement with the averages found from individual cases.

The shift toward higher frequency of the ΔT spectral maximum may be explained if we consider coherence and phase angle between 4-m and 8-m temperature. Coherence behaves like the square of the correlation coefficient between two time series, as a function of frequency. That is, at a given frequency coherence is unity for perfect correlation, $r=1$, unity for perfect anticorrelation, $r=-1$ (equivalent to 180-degree phase shift), and zero for no correlation, $r=0$. Thus we may regard coherence as the correlation of two signals as a function of frequency without regard to any phase shift that may be present.

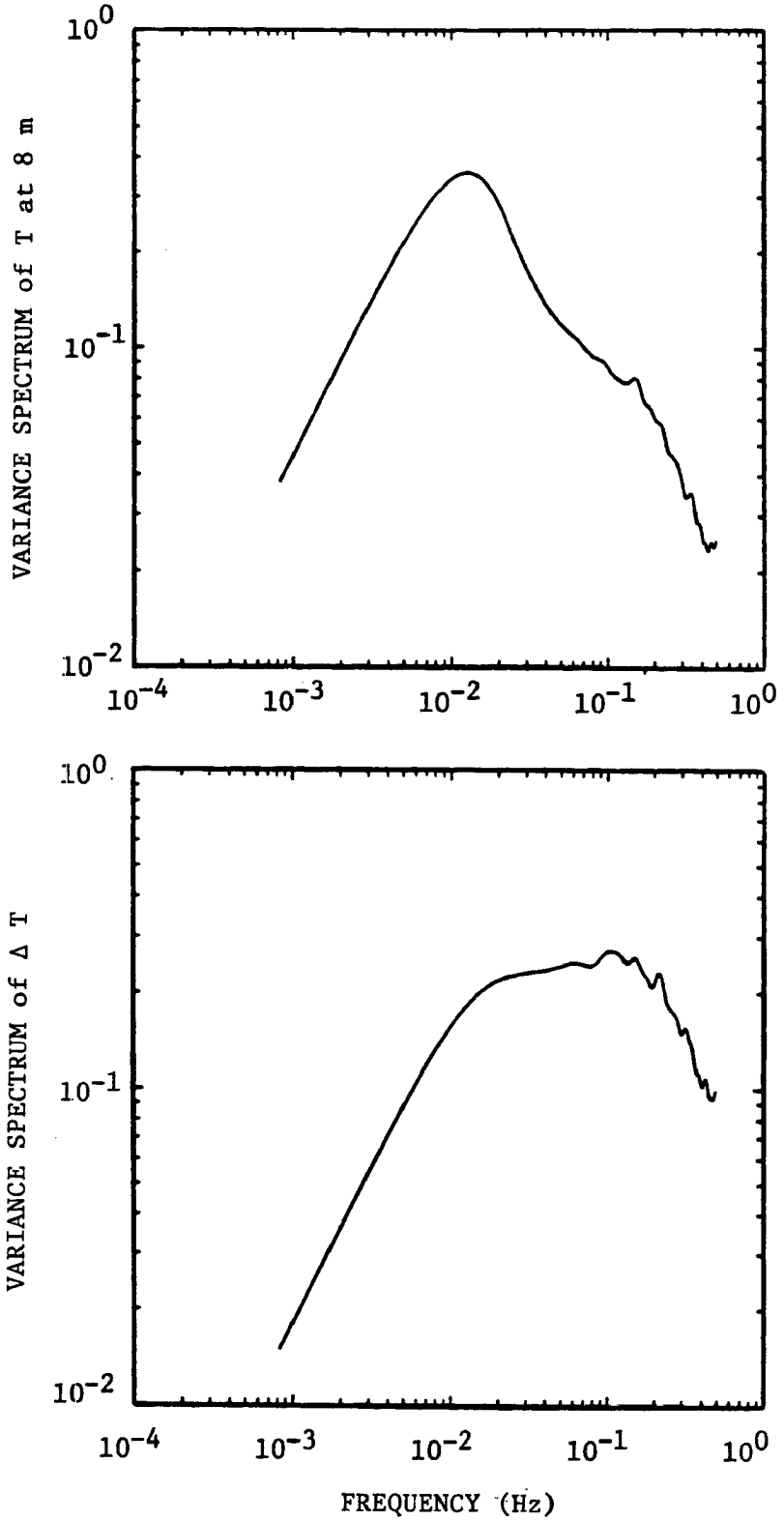

Figure 5. Composite spectral plots of T (8 m) and ΔT (8 m - 4 m). Each plot is a composite of normalized spectra for 21 cases of 1.2 ks (20 min). The spectral peak for ΔT is shifted toward higher frequency relative to the peak for T, probably due to the high coherence at low frequencies.

Composite coherence and phase angle were computed for the 21 cases used earlier to form composite spectra. Program SPECFT produced plots for the individual cases; these were averaged by frequency band to form the composites presented in Figure 6. The composite plots indicate that coherence is high (0.8) and the phase shift is zero for frequencies below 0.01 Hz, so that the time series are strongly correlated for $0<f<0.01$ Hz. The fact that the two time series closely follow each other in this frequency range implies that the variance of the difference time series must be small in this range. Thus the variance spectrum of ΔT at the lower frequencies must be depressed relative to the spectrum of T, which is confirmed by the spectra of Figure 5. This effectively moves the ΔT spectral maximum to the right, toward higher frequency and, hence, shorter time scale.

Having found the average time scales τ and τ_Δ for these 21 cases it is desirable to find generalized timescales τ_* and $\tau_{\Delta*}$ that allow these results to be applied under other conditions of stability, wind speed, and measurement height. We already have a general, dimensionless time scale τ_* (Eq 4), derived from the generalized temperature spectrum; now we wish to find a companion timescale $\tau_{\Delta*}$ for ΔT. The generalized temperature spectrum indicates that the frequency of spectral maximum is a function of stability. The SLACE data subset was acquired under unstable conditions in the range

$$-.8 \leq (z/L) \leq -.2, \quad z = 8 \text{ m}, \tag{5}$$

therefore generalization outside this range is not possible.

The scaling of the time scale at one level is given by (4) as $\tau=\tau_* z/\bar{u}$. It makes sense that τ scales with $1/\bar{u}$ because as wind speed increases eddies pass the sensor more rapidly, leading to shorter time

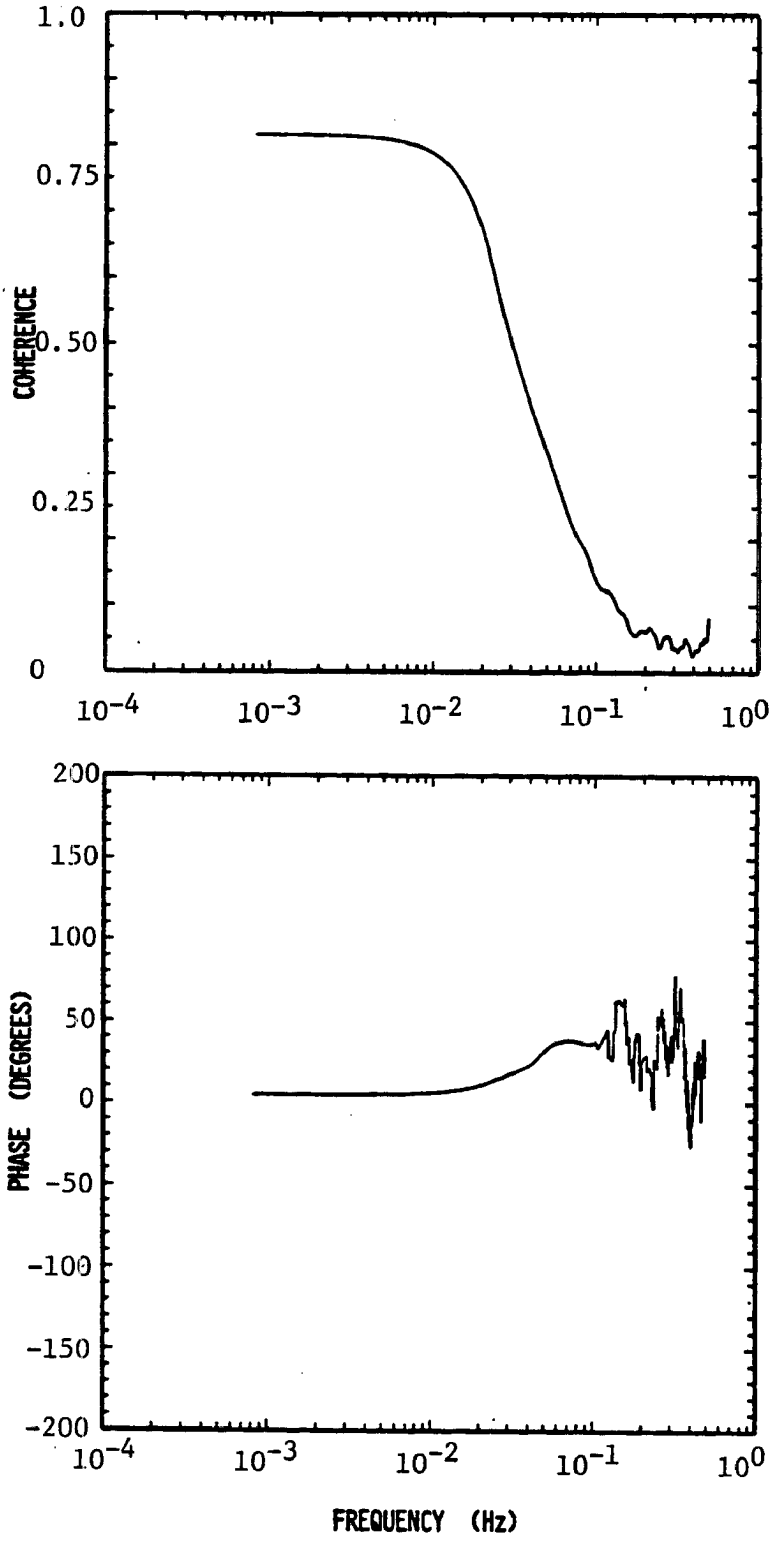

Figure 6. Composite coherence and phase angle between 8-m and 4-m temperature. Each plot is a composite of 21 cases of 1.2 ks (20 min). High coherence with zero phase angle indicates that the two time series are strongly correlated for frequencies below 0.01 Hz.

scale. Also, we can see that τ scales with z because as z increases the size of the largest eddies increases, leading to longer time scale.

Turning to the time scale of a difference, we may similarly define a dimensionless time scale $\tau_{\Delta *}$ such that $\tau_{\Delta}=\tau_{\Delta *}C$, where C (in seconds) is the ratio of a length scale and a velocity scale. The velocity scale is wind speed over the height interval Δz. To see this, consider that the time series of ΔT may be interpreted as gradient fluctuations being swept past the sensors by the mean wind. The spectral peak of ΔT is at the frequency that contributes most to the variance. Higher wind speed makes the gradient fluctuations pass more quickly (shorter time scale), therefore τ_{Δ} scales with $1/\bar{u}$.

For the length scale of τ_{Δ} we clearly cannot use z because of the ambiguity in the meaning of z for a difference measured between two heights; we will see that the appropriate length scale is Δz. Davenport [1961] hypothesized that in near-neutral stability the coherence of wind speed components at two heights is a function only of a dimensionless frequency interval

$$\Delta n = f(\Delta z)/\bar{u}$$

where Δz is the vertical separation and $\bar{u}$ is the mean wind speed in the layer. Pielke and Panofsky [1970] experimentally confirmed this hypothesis and found that the functional form is

$$coh(\Delta n) = \exp(-a\Delta n)$$

where a is a "decay parameter" dependent on stability. Thus wind-speed coherence falls off exponentially with vertical separation, and it is reasonable to assume that scalar coherence behaves similarly. Recall that low-frequency coherence causes the spectral maximum of ΔT to shift toward higher frequency (shorter timescale) relative to the spectrum of

T alone. If vertical separation is increased, then coherence is reduced and the ΔT spectral peak is shifted toward lower frequency (longer time scale); therefore τ_Δ scales with Δz. In the limit of very small Δz, τ_Δ approaches zero; in the limit of large Δz, presumably $\tau_\Delta = \tau$. Finally we have for the dimensionless time scale

$$\tau_{\Delta *} = \tau_\Delta \bar{u}/\Delta z \tag{6}$$

where $\bar{u}$ is the mean wind speed in the interval Δz.

The generalized time scales defined by (4) and (6) may now be estimated using the subset of temperature data described in Appendix B. For the 21-case averages we have $\tau \approx 80$ s and $\bar{u}(8.9\text{ m}) = 2.5\text{ m s}^{-1}$, giving for the temperature time scale $\tau_* = \tau\bar{u}/z \approx 20$. To evaluate the ΔT time scale we approximate the mean wind in the layer by the wind at $z = \sqrt{z_1 z_2} = 6.4$ m. Using $\tau_\Delta \approx 20$ s, $\bar{u}(6.4\text{ m}) = 2.4\text{ m s}^{-1}$, and $\Delta z = 4.2$ m we have $\tau_{\Delta *} = \tau_\Delta \bar{u}/\Delta z \approx 10$. (Because wind speed data are not available below 10 m the wind speeds were estimated using the diabatic wind profile; see Appendix B for details.) To use these dimensionless time scales in practice requires only that they be multiplied by the appropriate scaling factor (ie. $\tau_* z/\bar{u} = \tau$ or $\tau_{\Delta *}\Delta z/\bar{u} = \tau_\Delta$). Besides the obvious limitation that these values were obtained from 21 cases, the only other caveat attending their use is that they apply to stability conditions in the range (5).

Error Estimate for Two Sensors

Having arrived at an estimate for the time scale of ΔT, it is now possible to evaluate the averaging time equation (3), repeated here for convenience:

$$\varepsilon_a^2 = (\sigma_{\Delta T}/\langle \Delta T \rangle)^2 \approx (2/5)(\tau_\Delta/t_a)\overline{(\Delta T)'^2}/\overline{\Delta T}^2$$

We have estimates for all factors except the ratio, variance to

mean-squared, but this can be evaluated directly from the available data. This ratio was averaged over the subset of N=21 cases described in Appendix B with the result

$$(1/N) \sum [\ \overline{(\Delta T)'^2}/\overline{\Delta T}^2\ ] \approx 0.4 \qquad (7)$$

Using this value along with τ_Δ=20s and t_a=1.8 ks we have

$$\varepsilon_a \approx 0.04 \qquad (8)$$

If we assume a Gaussian distribution, then (8) means that, under the average conditions of the SLACE field study, a vertical gradient measurement made with a perfectly-matched pair of instruments has a 68% chance of falling within ±4% of the ensemble mean vertical gradient. The averaging time equation may be used to estimate sampling error due to limited averaging time under any set of field conditions, using either known or estimated values for the right-hand-side variables.

3. GRADIENT ERROR WITH ONE SENSOR USING INTERMITTENT SAMPLING

In the previous chapter we saw that a gradient measurement will include sampling error regardless of the measurement method. Now we turn to another form of sampling error, that introduced when intermittent sampling is used to measure the vertical gradient. It is shown that, in addition to the timescale τ, certain other timescales are important to the error level of an intermittent sampling system. These include the length of the down and up sampling cycle, the transit time between levels, and the response time of the instrument in responding to a change of level. This chapter begins with a general discussion of why and how this error comes about, followed by a description of the empirical approach used to quantify the error. Results are given for an idealized (instantaneous) intermittent sampling system, and then are extended to include real sampling systems with finite transit and instrument response times. Finally, an estimate of total sampling error is made by combining the contributions of intermittent sampling error and averaging time error.

Obviously, disregarding half the data available to determine the gradient, as we must do when we sample intermittently at two levels, is a source of sampling error. The nature of this kind of sampling error becomes clearer when we consider two hypothetical cases. The first case is illustrated in Figure 7, where a linear trend is present in the data. The two traces shown might be from temperature sensors during the

morning hours, showing the expected temperature increase. Clearly there are two data sets: the one "seen" by the intermittent sampler, indicated by the darkened segments in the figure; and the one "thrown away." Either one of these datasets is available simply by choosing down or up as the starting position. But because the down and up sampling periods are offset in time, the consequence of having a trend in scalar concentration is that the two datasets give different gradient results: selecting 4 m first underestimates the gradient, 8 m first overestimates it. This problem can be avoided by removing the linear trend from the data prior to calculating the gradient.

The nature of intermittent sampling error is further illustrated in the following thought-experiment. We shall pretend that we have a positive mean gradient in an ultra-simplified form of turbulent flow where all the eddies are the same size. Also, we shall set the timer of our elevator mechanism to complete one down/up cycle in the same time it takes for a single eddy to pass the tower. The situation is shown in Figure 8. Again we ask, Is the result different if we start in the down position first, or the up position? Ideally the results ought to be insensitive to this choice, but as Figure 8 shows, the results can be divergent. This simplified example shows how sampling error can affect the difference measurement, but it also shows that the timing of the sampling cycle relative to the time for eddies to pass the tower must be considered in the design of a vertical difference experiment.

It is interesting to note that because the intermittent sampling system uses half the data of a two-instrument measurement, using either half of the data (down-first or up-first) produces errors that are symmetric about the two-instrument result. That is, the gradient

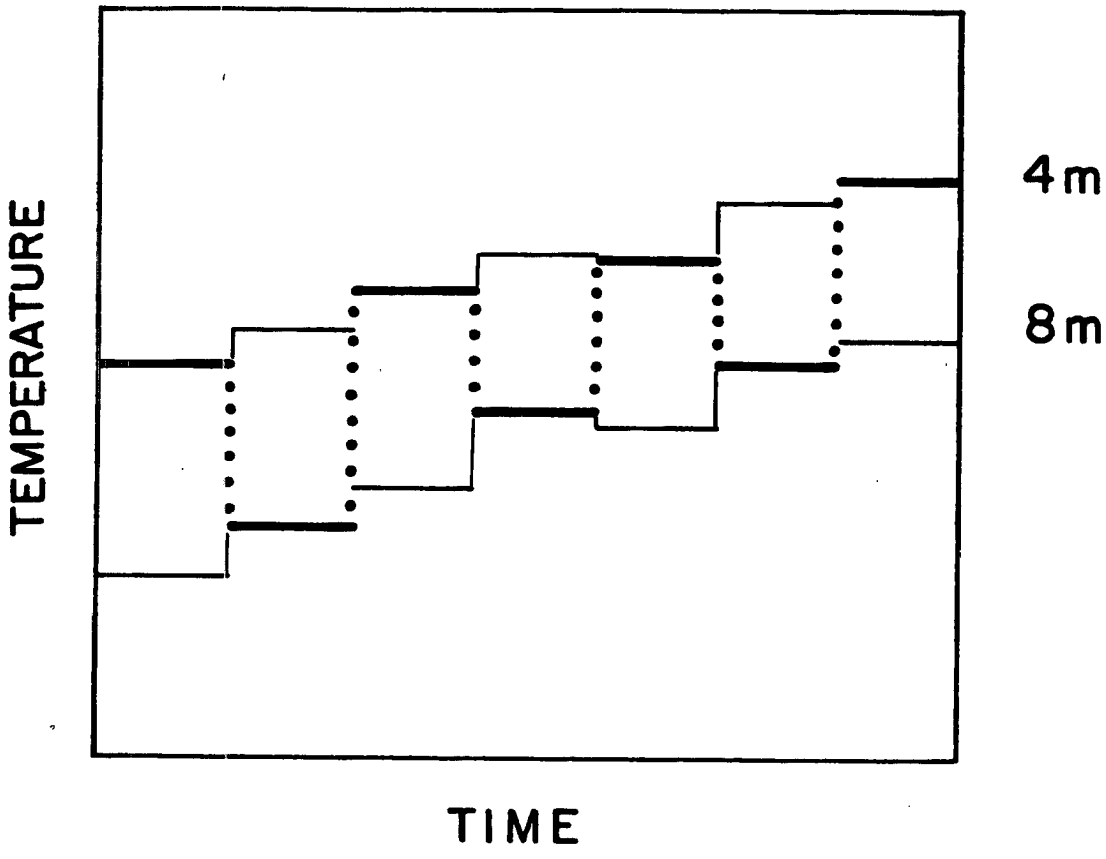

Figure 7. Example of gradient data with linear trend. Mean values for intermediate periods are indicated as horizontal lines. Computed gradient is sensitive to the choice of starting position.

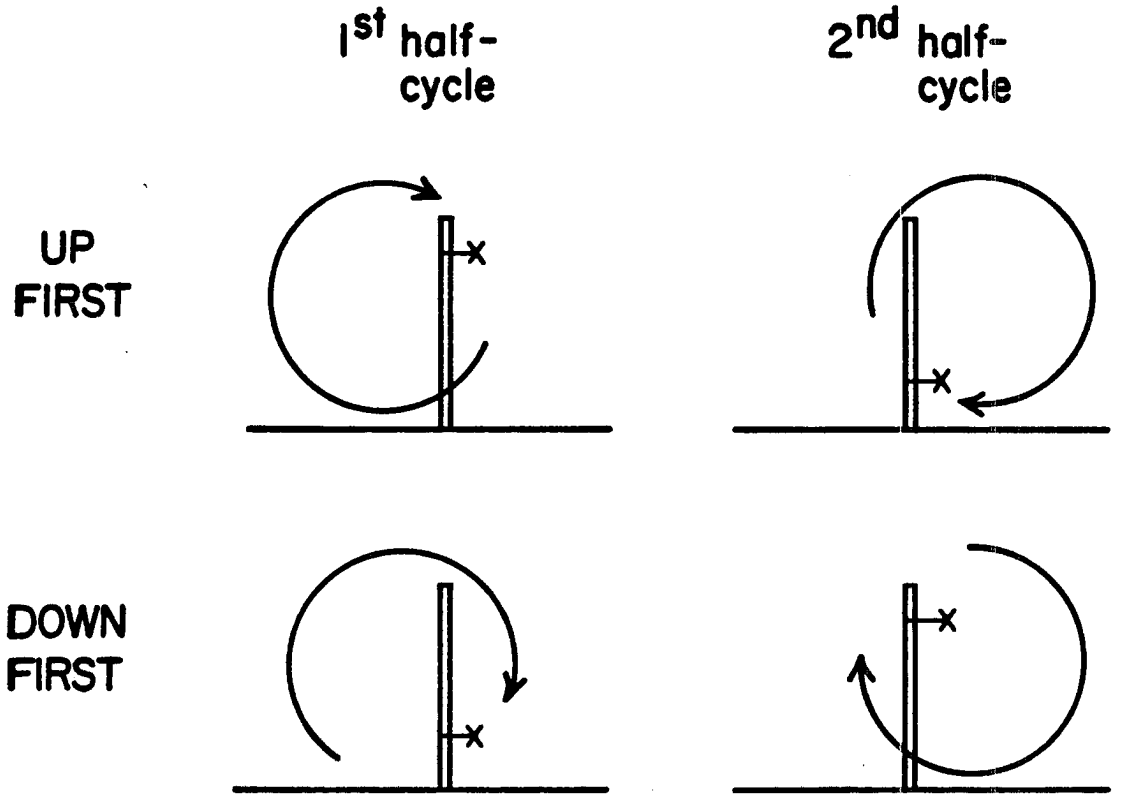

Figure 8. Sensitivity to starting position. Hypothetical turbulence has only one eddy size and eddies pass the tower in the same time as one down-and-up cycle. If sampling begins in the up position, air with higher-than-average concentration moves past the sensor during the first half-cycle, because average concentration increases with height. During the second half-cycle the sensor records lower-than-average concentration and subtracting the two results gives a positive gradient. But if sampling begins in the down position, higher concentration is brought down to the sensor in the first half-cycle and, in the second half-cycle, lower concentration is brought to the sensor in the up position. Now the observed gradient is smaller than before and may even be negative, contradicting the stipulated upward gradient.

results obtained when starting in the down or up position deviate from the two-instrument result by amounts that are equal but opposite in sign. Also it can be shown for idealized instruments that the average of the up-first and down-first results is identically equal to the two-instrument result. This fact suggests yet another approach to measuring a gradient, a combination using two instruments AND intermittent sampling. In this method two sensors or sample inlets exchange positions periodically, the gradient is computed separately from the intermittent data record of each instrument, and the results are then averaged. This hybrid method combines the advantage of using a single instrument (elimination of intercalibration problems) with the advantage of using two instruments (full use of the available data); it requires only that instrument calibration does not change or drift during a run. This method has been used successfully by Droppo [1985] in an experiment to measure the surface flux of ozone. Its use is suggested whenever the required equipment is available, ie., two similar instruments and apparatus for intermittent sampling (an elevator or an alternating valve). The error of this system is not sensitive to the ratio of cycle time to time scale of the signal because it attains full coverage of the available data, excepting only the data lost during transitions. It can be shown that, for a system with instantaneous transition time, the gradient result is identical for any cycle time. Therefore a real system can be operated with only one exchange of positions during each run, thus minimizing data lost to transitions.

Sampling Error in an Idealized Intermittent System

To obtain an estimate of the error introduced when sampling a vertical gradient intermittently, the temperature gradient data set described in Chapter 2 was pressed into service. Since continuous records are available at 8 m and 4 m, we can "sample" alternately from the two time series and thus simulate the action of an intermittent gradient sampling system. We can then compare the gradient result from intermittent sampling with the gradient computed using the full data record. Figure 9 illustrates the technique. By varying the probe cycle time we can determine its effect on sampling error. Recall that the temperature gradient dataset is divided into 42 cases of 1.8 ks (30 min) length and that all data were obtained under unstable conditions. The simulation was performed for each case using 12 different probe cycle times. For each probe cycle time the relative error was calculated as the mean deviation

$$\varepsilon_I = (1/N) \sum |(\Delta T_I - \Delta T_C)/\Delta T_C| \qquad (9)$$

where ΔT_I and ΔT_C are the temperature gradients computed from intermittent and continuous data, respectively, and N=42.

In the first simulations an idealized sampling system was assumed, ie., an elevator that changes levels instantly and an instrument that responds instantaneously to concentration changes. The scatter plot in Figure 10 shows the result of the simulations prior to averaging by (9). It is readily apparent that the results for a given cycle length are spread over at least two orders of magnitude and that the error level tends to increase with cycle time. After applying (9) to find the mean deviation for each cycle time we have the result summarized in Figure 2 (page 13): the relative error increases monotonically with cycle time

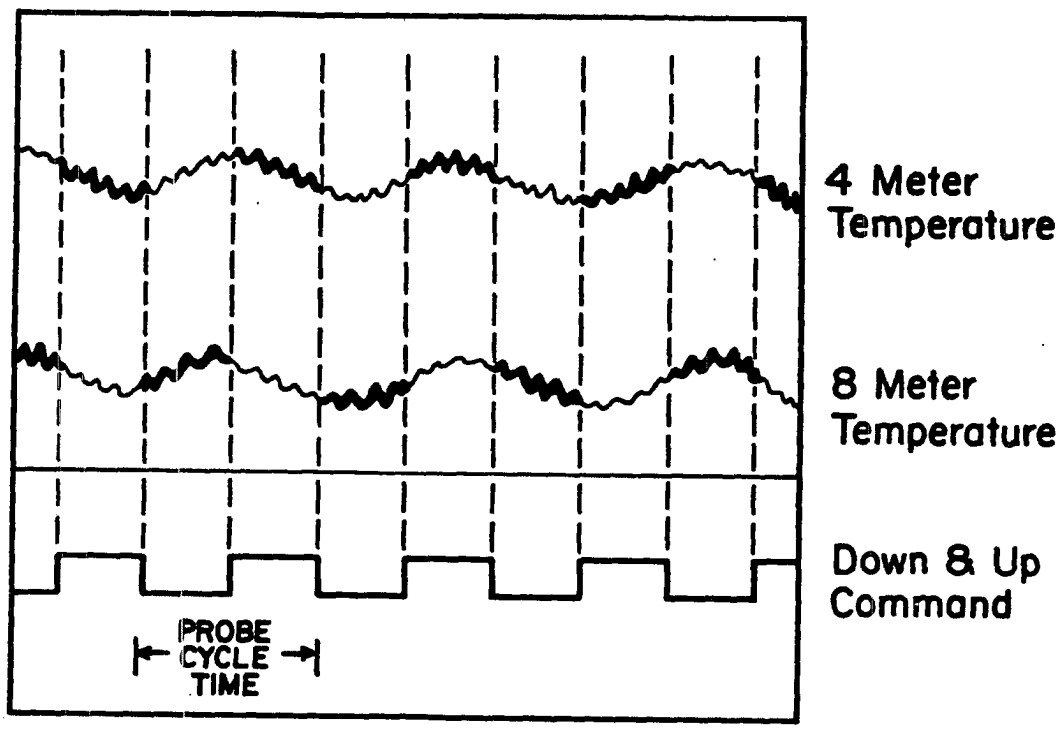

Figure 9. Simulation of intermittent gradient sampling using continuous data. Darkened segments show how an intermittent data record is extracted from two continuous time series, in response to a simulated command channel. Probe cycle time can be systematically varied to learn its effect on sampling error.

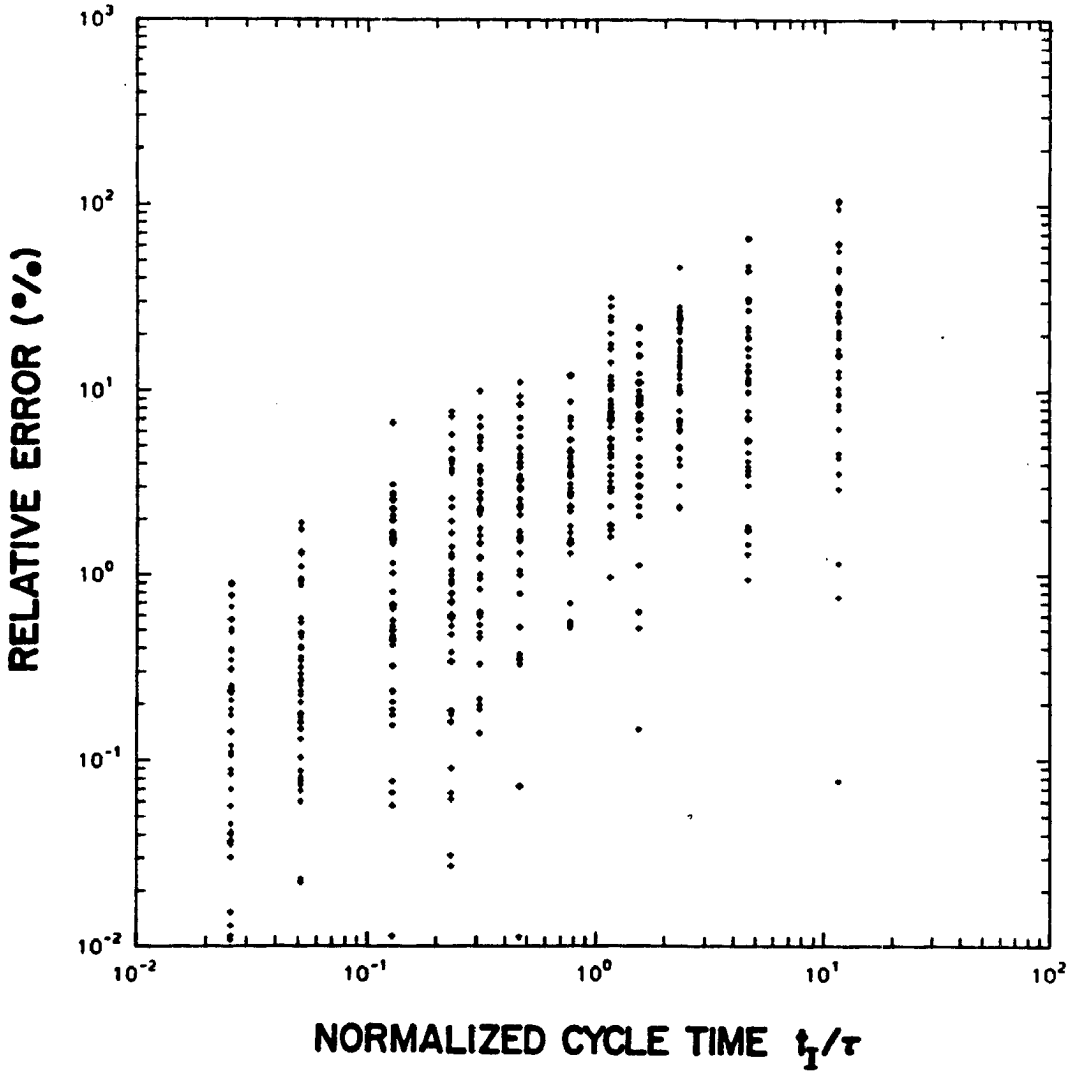

Figure 10. Scatter plot of relative error (%) as a function of cycle time. The abscissa is cycle time normalized by timescale τ=80. For each cycle time there are 42 points, each giving the relative error for a single simulation.

according to the relation

$$\varepsilon_I = 6(t_I/\tau)^{0.8} \qquad (10)$$

where cycle time has been normalized by the timescale of the upper temperature time series, $\tau = 80$ s. Note that τ, not τ_Δ, normalizes the cycle time: we saw in Figure 8 that sampling error is sensitive to the relationship of cycle time to the time scale of passing eddies, not to the time scale of vertical difference. The conclusion we may draw from (10), and the principal finding of this study, is that if we wish to minimize error in a gradient measurement we must use the smallest cycle time that can be achieved. For example, since the temperature timescale of the the SLACE field study was about 80 s, and the cycle time was 360 s (6 min), evaluation of (10) gives an error rate of 20%. If we wanted to reduce this to around 1% error we would have to reduce the cycle time to around 8 s (4 s up, 4 s down). Clearly, in a real experiment there is a practical limit to how frequently one can cycle up and down, the limit imposed by the finite response time of the instruments and the finite transit time between levels.

Sampling Error in a Real Intermittent System

At every height transition some data must be blanked out while the elevator is in motion and while instrument output approaches a stable value at the new level. The data that is lost at the height transitions clearly must contribute something to the error of an intermittent gradient measurement.

An additional delay time in a gas sampling system is the plumbing lag, or the time for gas to travel from inlet on the tower to inlet of the gas sampler. However if the gas stream may be approximated as plug flow, this plumbing lag is constant and may be easily accommodated

during data reduction by applying a constant time offset to instrument output relative to transition events at the tower inlet. One may assume that a gas approximates plug flow if the flow is turbulent, ie., if the Reynolds number $R_e = DV\rho/\mu > 2000$, where D and V are diameter and velocity in the inlet line, ρ and μ are air density and viscosity.

To determine the contribution of "dead time" to error in an intermittent measurement further simulations were done, this time varying the amount of dead time at each height transition as well as the probe cycle time. Figure 11 summarizes the result of the simulations. At the left edge of the figure are the results for zero deadtime, the same values that were displayed in Figure 2 (page 13), indicating that error increases with cycle time. As an example, let us begin with zero blanking at a cycle time that produces a 4% error. Moving to the right into regions of increased blanking time, the error also increases until we reach a blanking rate of 0.8 with an error of 8%. At this point we have thrown away nearly all the data by blanking, but the error rate has merely doubled. This example illustrates the general result: since the slope of the isopleths is small the choice of cycle time is much more significant in determining the error of an intermittent gradient measurement than is the fraction of each cycle lost in blanking.

Evaluation of Dead Time

Practical use of Figure 11 requires an estimate of the blanking time t_0 which is a function of instrument response time t_r and elevator transit time t_e. If $t_r >> t_e$ or if $t_r << t_e$, then t_0 may be estimated simply as the dominant timescale. But in the usual situation where $t_r \sim t_e$, the combination of the two time scales is more complicated.

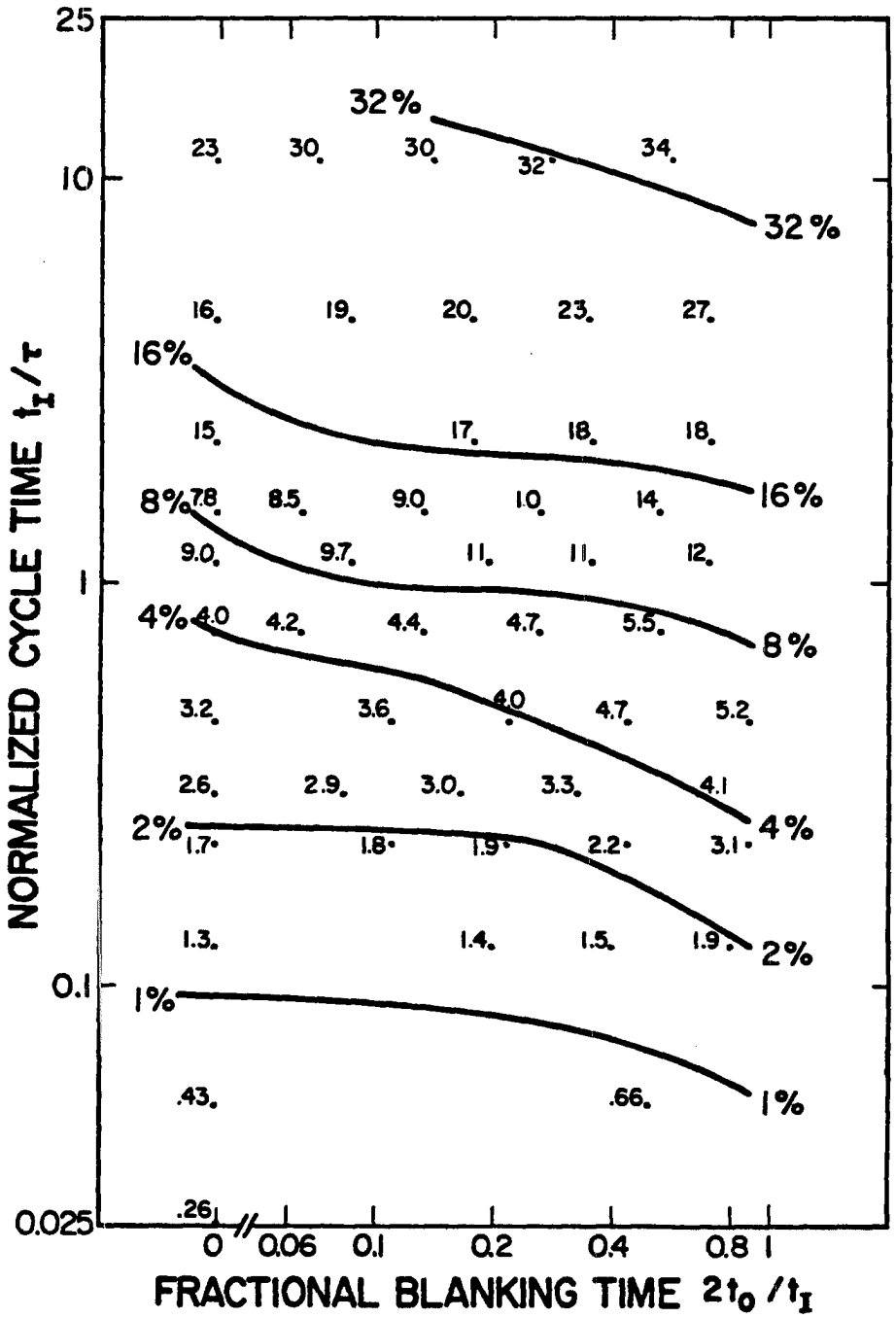

Figure 11. Relative error of an intermittent gradient measurement as a function of cycle time and blanking time. Ordinate is probe cycle time normalized by the timescale of the upper temperature time series, abscissa is the fraction of each cycle lost to blanking (t_0 seconds at each height transition). Each data point is the mean deviation (%) for 42 cases. Curves are isopleths of constant error. The moderate slope of the isopleths indicates that the choice of cycle time contributes much more strongly to the error rate than does the fraction of a cycle lost to blanking.

An estimate of the blanking time can be obtained analytically. The response E_o of a gas monitoring instrument to a step change in concentration E_i may usually be characterized as exponential decay. The instrument reponse time t_r is the time required for the displacement E_o-E_i to be reduced to 1/e times its initial value (the e-folding time). For such an instrument E_o and E_i are related [Kaplan, 1981] by

$$(dE_o/dt) + (E_o/t_r) = E_i/t_r \qquad (11)$$

If we specify how the gas concentration $E_i(t)$ changes during a height transition, then we may solve (11) to find the time required for E_o to approach arbitrarily close to the new level concentration.

The mean profile of a scalar is logarithmic with height in the surface layer. If the curvature of the profile is very strong it is conceivable that t_0 may have hysteresis, that is, the combined system response time could depend on the direction the elevator is going. However, to simplify this analysis we shall assume that the concentration increases linearly with height and that the concentration is zero at the lower level. Given these conditions the behavior of E_i during and following a height transition is illustrated by the ramp function of Figure 12. The solution to (11) for the forcing function of Figure 12 is found in Appendix C to be

$$\begin{aligned} E_o/E_1 &= 1 - A\exp(-t/t_r) \\ A &= (t_r/t_e)\,[\exp(t_e/t_r) - 1] \end{aligned} \qquad (12)$$

If we now set $E_o/E_1 = (1 - e^{-n})$, then we may solve (12) for the time to reduce the initial displacement E_1 by n-fold factors of e. After making this substitution and solving for $t=t_0$ we have

$$t_0 = t_r n + t_r \ln\{(t_r/t_e)[\exp(t_e/t_r) - 1]\} \qquad (13)$$

A practical choice is n=2 (giving $E_o/E_1=0.86$); then t_0 is the time for

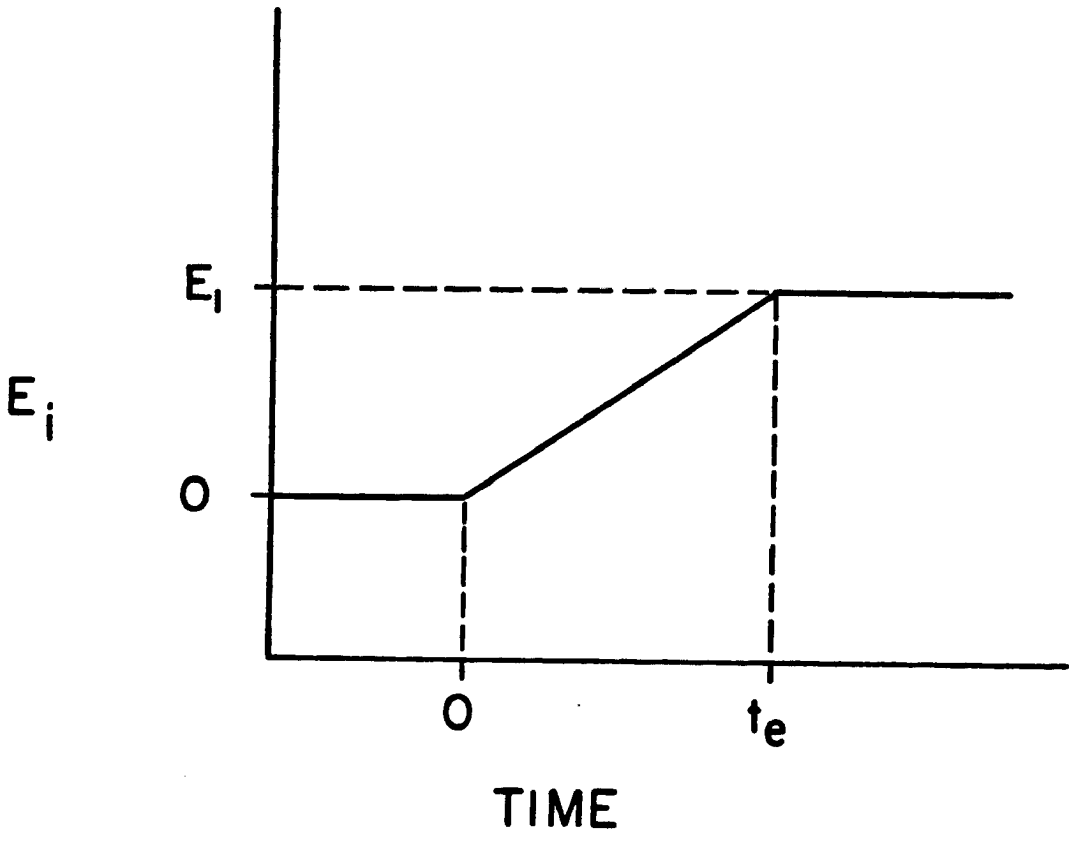

Figure 12. Ramp forcing function. Gas concentration is zero initially. At onset of height transition (t=0) concentration increases linearly to E_1 at the new level, after transition time t_e.

E_o to achieve 86% of its final value after the height transition. Figure 13 shows the result of evaluating (13) for n=2: the figure may be used to estimate the dead time for any combination of transit time t_e and instrument response time t_r.

Combined Sampling Error

In Chapter 2 we found an expression for the relative error ε_a of a gradient measurement made with dual instrumentation. In the last section we found the error ε_I (mean deviation) of estimating the dual-instrument gradient using an intermittent sampling scheme. Many investigators would wish to know how these two forms of sampling error contribute to the total error in making a vertical gradient measurement, but before discussing how they might combine it is well to clarify the meaning of ε_a and ε_I.

Recall that ε_a is the standard error of estimating the ensemble mean by sampling a single realization of the flow over averaging time t_a. We may visualize an enormous, flat plain with uniform ground cover and sampling sites on, say, a 1-km grid. Each sampling site has an instrument that accurately measures the instantaneous vertical gradient s. Average conditions (L, u, heat flux, etc.) are identical at each site. Now if all the sites do a simultaneous sampling run of length t_a, then the average of the mean gradients $\bar{s}$ at all sites is the ensemble mean $\langle s \rangle$, the individual site means are distributed around the ensemble mean with standard deviation σ_a, and the standard error of the site means is $\varepsilon_a = \sigma_a/\langle s \rangle$. If we now select a single measuring site from our grid, we know that the local mean $\bar{s}$ is the correct value of the gradient at that site for a single run (though it may deviate from the ensemble mean). Suppose we equip this site with a second gradient

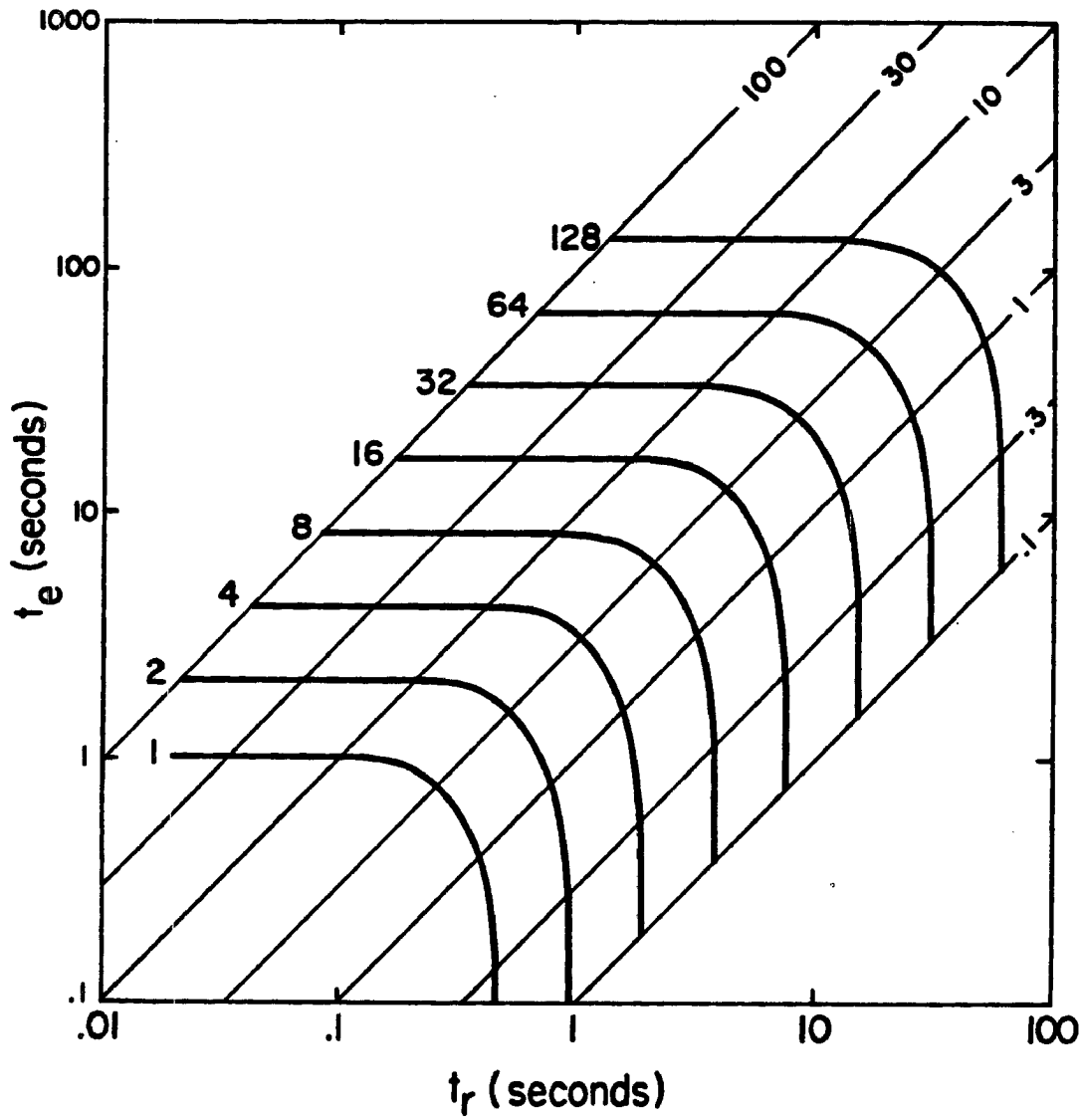

Figure 13. Dead time, or time for instrument to achieve 86% of its final value following height transition. t_r is the e-folding time of the instrument, t_e is the transit time of the elevator. The curves are isopleths of constant deadtime t_0, in seconds. Values of the ratio t_e/t_r are shown as straight lines.

measurement system that samples intermittently. After many runs we would find that the gradient values obtained with this second system deviate from $\bar{s}$ by ε_I, on average.

Thus the two error contributions are formulated differently, and can not be conveniently combined to give a total sampling error. While it might be desirable to find a statistically meaningful formulation for the intermittent gradient measurements about the ensemble mean gradient, we may do so only if the intermittent sampling errors are normally distributed and if the intermittent sampling error is formulated as a standard deviation or standard error. However it has not been shown that the intermittent error values follow a Gaussian distribution and we must therefore content ourselves with a less formal approach to combining these two forms of sampling error.

For the investigator who wishes to have an estimate of the standard error of intermittent gradient measurements about the ensemble mean gradient, two models should be considered. The additive model

$$\varepsilon = \varepsilon_a + \varepsilon_I \tag{14}$$

corresponds to a worst-case estimate, since it applies to situations where the errors are deterministic (have no random component). In situations where the errors have a stochastic (random) component, and if the error variances are not correlated (deviations from the mean values are not correlated), then the second model applies:

$$\varepsilon^2 = \varepsilon_a^2 + \varepsilon_I^2 \tag{15}$$

This model gives smaller values for the total sampling error, but it is strictly correct only if ε_a and ε_I are standard errors, which ε_I is not. Still, both these errors have a stochastic component, so the best estimate probably lies between (14) and (15). The conservative approach is

to estimate the combined sampling error as their sum, ie., (14). In practice ε_a is the dominant term when the intermittent sampling cycle is short ($t_I/\tau<0.5$), while the intermittent sampling error dominates for longer cycle times.

4. CONCLUSION

Experiments that measure vertical concentration differences in the surface layer are becoming common with the increasing interest in dry deposition studies. Investigators who have attempted to overcome measurement error by sampling alternately at two levels with a single instrument have encountered sampling error. This study uses continuous temperature measurements made at two levels to determine empirically the sampling error of a one-instrument temperature gradient measurement. The results may be used to estimate the sampling error of past and future one-instrument gradient measurements.

Two forms of sampling error occur in such a measurement; each is a function of a time scale of the experimental procedure and a time scale of the surface layer turbulence within which the measurement is made. Generalized dimensionless time scales have been found for scalars ($\tau_* \approx 20$) and for scalar differences ($\tau_{\Delta *} \approx 10$), when atmospheric stability falls in the range $-.8 < (z/L) < -.2$. These may be used to estimate the local time scale of any scalar ($\tau = \tau_* z/\bar{u}$) or its gradient ($\tau_\Delta = \tau_{\Delta *} \Delta z/\bar{u}$). These time scales, although derived from temperature spectra, are applicable to all scalars.

The basic sampling error present in any measurement of a mean quantity $\bar{s}$ in turbulent flow is given by a simplified averaging time equation

$$\varepsilon_a^2 = (\sigma_s/\langle s \rangle)^2 \approx (2/5)(\tau/t_a)\overline{s'^2}/\bar{s}^2$$

For $s=\Delta T$ the average conditions of the SLACE field study give $\varepsilon_a \approx 4\%$. This equation may be evaluated for any scalar difference measurement, given an estimate of the time scale, variance, and mean of the difference time series.

The second form of sampling error is due to intermittent sampling at two levels. It has been shown by simulation of intermittent sampling between two continuous temperature time series that sampling error increases monotonically with probe cycle time. The mean deviation (%) of the simulated gradients about the continuous gradients obeys the relation

$$\varepsilon_I = 6(t_I/\tau)^{0.8} \tag{5}$$

for an idealized system with zero dead time. When the finite instrument response time and transit time of a real system are used in the simulations, sampling error still depends strongly on cycle time with a much weaker dependence on dead time. Figures 9 and 11 may be used to estimate ε_I for any combination of instrument response time, transit time, and probe cycle time. The combined sampling error of a one-instrument gradient measurement relative to the ensemble mean gradient is

$$\varepsilon \leq \varepsilon_a + \varepsilon_I$$

where the equal sign is used in a conservative approach. The one-instrument gradient measurements during SLACE were subject to a combined error of 24%.

REFERENCES

Bendat, J. S., and A. G. Piersol, 1971: Random data: analysis and measurement procedures, 407 pp., Wiley-Interscience, New York.

Blackman, R. B., and J. W. Tukey, 1958: The measurement of power spectra, Dover Publications, New York.

Businger, J. A., J. C. Wyngaard, Y. Izumi, and E. F. Bradley, 1971: Flux-profile relationships in the atmospheric surface layer, J. Atmos. Sci. 28, 181-189.

Davenport, A. G., 1961: The spectrum of horizontal gustiness in high winds, Quart. J. Roy. Meteor. Soc. 87, 194-211.

Davis, C. S., and R. G. Wright, 1985: Sulfur dioxide deposition velocity by a concentration gradient measurement system, J. Geophys. Res. 90(D1), 2091-2095.

Delany, A. C., R. R. Dickerson, F. L. Melchoir, and A. F. Wartburg, 1982: Modification of a commercial NO_x detector for high sensitivity, Rev. Sci. Instrum. 53, 1899-1902.

Delany, A. C., and T. D. Davies, 1983: Dry deposition of NO_x to grass in rural East Anglia, Atmos. Environ. 17, 1391-1394.

Dolske, D. A., and D. F. Gatz, 1985: A field intercomparison of methods for the measurement of particle and gas dry deposition, J. Geophys. Res. 90(D1), 2076-2084.

Droppo, J. G., Jr., 1985: Concurrent measurements of ozone dry deposition using eddy correlation and profile flux methods, J. Geophys. Res. 90(D1), 2111-2118.

Fitzjarrald, D. R., and D. H. Lenschow, 1983: Mean concentration and flux profiles for chemically reactive species in the atmospheric surface layer, Atmos. Environ. 17, 2505-2512.

Garratt, J. R., 1980: Surface influence upon vertical profiles in the atmospheric near-surface layer, Quart. J. Roy. Meteor. Soc. 106, 803-819.

Hicks, B. B., and M. L. Wesely, 1978: An examination of some micrometeorological methods for measuring dry deposition, EPA-600/7-78-116, U. S. Environmental Protection Agency, July 1978.

Hicks, B. B., M. L. Wesely, and J. L. Durham, 1980: Critique of methods to measure dry deposition, Workshop Summary, EPA-600/9-80-050, U. S. Environmental Protection Agency, Research Triangle Park, NC, Sept. 1980.

Holloway, J. L., Jr., 1958: Smoothing and filtering of time series and space fields, in Advances in Geophysics, IV, edited by H. E. Landsberg and J. van Mieghem, pp. 351-389, Academic Press, New York.

Kaimal, J. C., 1975: Sensors and techniques for direct measurement of turbulent fluxes and profiles in the atmospheric surface layer, Atmos. Technol. 7, 7-14.

Kaimal, J. C., and J. E. Gaynor, 1983: The Boulder Atmospheric Observatory, J. Climate Appl. Meteor. 22, 863-880.

Kaimal, J. C., J. C. Wyngaard, Y. Izumi, and O. R. Cote, 1972: Spectral characteristics of surface layer turbulence, Quart. J. Roy. Meteor. Soc. 98, 563-589.

Kaplan, W., 1981: Advanced Mathematics for Engineers, 927 pp., Addison-Wesley, Reading, Massachusetts, 1981.

Lenschow, D. H., 1982: Reactive trace species in the boundary layer from a micrometeorological perspective, J. Met. Soc. Jap. 60, 472-480.

Liepman, H. W., 1952: Aspects of the turbulence problem, Z. F. Angew. Math. U. Phys. 3, 321-342.

Lumley, J. L., and H. A. Panofsky, 1964: The structure of atmospheric turbulence, John Wiley and Sons, New York.

Panofsky, H. A., and J. A. Dutton, 1984: Atmospheric turbulence, models and methods for engineering applications, 397 pp., Wiley-Interscience, New York.

Pearson, R., Jr., and D. H. Stedman, 1980: Instrumentation for fast response ozone measurements from aircraft, Atmos. Technol. 12, 51-55.

Pielke, R. A., and H. A. Panofsky, 1970: Turbulence characteristics along several towers, Boundary Layer Meteorol. 1, 115-130.

Wendel, G. J., D. H. Stedman, C. A. Cantrell, and L. Damrauer, 1983: Luminol-based nitrogen-dioxide detector, Anal. Chem. 55, 937-940.

Willis, G. E., and C. A. Paulson, 1963: The measurement of mean vertical profiles of wind speed, temperature, and humidity over water surfaces, Part One of the Annual Report to the National Science Foundation covering research sponsored under grant G-21575, June, 1963.

APPENDIX A

THE SURFACE LAYER ATMOSPHERIC CHEMISTRY EXPERIMENT

The Surface Layer Atmospheric Chemistry Experiment (SLACE) was undertaken to independently measure the fluxes of O_3, NO, and NO_2 in the surface layer by both eddy correlation and gradient methods simultaneously. In addition, measurement of the photolytic rate constant j_{NO_2}, atmospheric moisture, and detailed hydrocarbon analyses were carried out, making this perhaps the most comprehensive experiment to date on the photochemistry of the surface layer.

SLACE is a cooperative venture involving investigators from the National Center for Atmospheric Research (NCAR), Colorado State University (CSU), Colorado College, The University of Michigan, and the National Oceanic and Atmospheric Administration (NOAA). One unique feature of this collaboration is the assembly of fast chemical instrumentation (10-Hz sampling rate) to measure O_3, NO, and NO_2 in a surface layer experiment.

Objectives

There are four principal objectives of SLACE. The first is to measure and compare the fluxes of O_3, NO, and NO_2. While O_3 flux is always downward or zero (there is no surface source of ozone), NO and NO_2 are respirated by plants and soil, and the net flux may be upward or downward depending on the diurnal growth cycle and on soil conditions. Delany et.al. [in preparation] document variations in the direction and

intensity of NO and NO_2 flux and propose an explanation of the underlying mechanisms.

The second objective is to improve the rigor of dry deposition measurement techniques by comparing the eddy correlation and gradient methods. Recent interest has prompted atmospheric chemists and micrometeorologists to reexamine the validity and potential of different techniques for the determination of surface deposition of atmospheric species. In the "Critique of Methods to Measure Dry Deposition: Workshop Summary" [Hicks et al., 1980], the eddy correlation technique for determination of the scalar flux $F_s=\overline{w's'}$ was established as being the most rigorous, although it was recognized that the technique is technically difficult as it requires the development of fast (~10 Hz) chemical sensors. The gradient technique $F_s=k_h(\Delta\bar{s}/\Delta z)$ was accepted as suitable, provided the turbulent flow is horizontally homogeneous. The second objective, more precisely, is to compare the results from these two methods and characterize any circumstances under which the two methods do not agree.

A third objective is to test the assumption that all scalar diffusivities are equal. It is commonly held by micrometeorologists that the diffusivity of any scalar is the same as that for heat, ie., $k_h=k_s$. The dataset obtained in the SLACE experiment should allow us to verify this assumption for heat, O_3, NO, and NO_2, since simultaneous eddy correlation and gradient measurements were obtained for each of these species.

Thus we may obtain eddy diffusivities independently for

heat $k_h = c_p \rho \overline{w'T'} / (\Delta\bar{\theta}/\Delta z)$,

ozone $k_{O_3} = \overline{w'O_3'} / (\Delta\overline{O_3}/\Delta z)$,

nitric oxide $k_{NO} = \overline{w'NO'} / (\Delta\overline{NO}/\Delta z)$, and

nitrogen dioxide $k_{NO_2} = \overline{w'NO_2'} / (\Delta\overline{NO_2}/\Delta z)$.

The fourth objective is to investigate the divergence/convergence of the flux of chemically reactive species in the surface layer. The surface layer is often referred to as the "constant flux layer" on the assumption that vertical flux is invariant with height. However, this assumption may be incorrect in the presence of chemical reactions. Lenschow [1982] shows that significant flux divergence may be expected when the time scales for chemical reactions and turbulent transport are the same order of magnitude. Fitzjarrald and Lenschow [1983] develop relations for the change of flux with height in the presence of reactions. They point out that flux estimates at the surface based on concentration measurements made at some height above the surface must take into account reactions that occur below the measurement height. For the photochemical reaction triad O_3, NO, and NO_x they conclude that to reliably obtain the flux of any of the three at least six measurements are required: each gas measured at two levels in the surface layer. Since the SLACE dataset includes the required six measurements their model may be compared with observations. Flux divergence was also investigated directly in the SLACE experiment by measuring the flux at two levels using the fast instruments and the eddy correlation technique. Simple comparison of the flux at two levels may verify the presence of flux divergence.

Roles of the Investigators

A. C. Delany, Atmospheric Chemistry and Aeronomy Division, National Center for Atmospheric Research (NCAR/ACAD): overall planning and coordination; supplied fast NO instrument, sonic annemometers, and most gradient instruments.

D. R. Fitzjarrald, Advanced Studies Program (NCAR/ASP): micrometeorology; analysis of data from fast instrumentation.

J. E. Gaynor, National Oceanic and Atmospheric Administration (NOAA): computer data acquisition at NOAA's Boulder Atmospheric Observatory (BAO); supplied dew point and fast water vapor instruments.

B. J. Hubert, Colorado College: measurement of nitric acid flux by the gradient method in a stand-alone experiment.

D. H. Lenschow, NCAR/MRS: planning and guidance on micrometeorology.

R. Pearson, Jr., Colorado State University: supplied fast ozone instrument; analysis of data from slow instrumentation.

D. Stedman, University of Denver: supplied fast NO_2 instrument.

The Research Site

The field work was carried out during May, June, and July, 1983, at the Boulder Atmospheric Observatory (BAO), operated by the National Oceanic and Atmospheric Administration (NOAA). The BAO is a research facility comprised of a 300-meter tower with eight levels of instrumentation, a data acquisition system, and support personnel. The site is about 30 km NNW of Denver, Colorado, and is characterized by moderately polluted air without local emission sources.

Several factors directed this choice of site for the SLACE experiment. Uniform terrain and ground cover with adequate fetch are critical

requirements of the gradient method for determining the chemical fluxes; the surface upwind of a measurement site must be flat and uniform out to 100 times the measurement height [Hicks and Wesely, 1978]. The BAO tower is on flat terrain and surrounded for about one kilometer in every direction by a planting of crested wheat grass, thus allowing measurements up to the 10-meter level. The data acquisition system at the BAO was an important plus: whereas the mobile data system designed for this project had not been proven in the field, the BAO data system could provide backup. This redundancy paid off as the mobile data system suffered many setbacks, and the backup system became crucial to the success of the project. The data from the permanent sensors located on the 300-meter tower, though not directly a part of SLACE, could be used to supplement measurements in the micro-regime at the surface, the focus of the experiment. Finally, NOAA's support personnel at the site could provide useful assistance with instruments and the data system.

Within the BAO grounds, the SLACE research site itself was located 150 meters from the base of the tower in order to avoid perturbations of the surface layer winds near the small buildings at the tower base. Two masts and two scaffolds were erected for instrumentation, as shown schematically in Figure 14. These structures were placed along a north-south line to expose instruments to the predominantly easterly daytime flow indicated by climatological records. The maximum height of measurement was about 9 m, consistent with the 10-m limit imposed by the upwind fetch requirement.

Two independent data acquisition systems were used, the BAO system which is in place at the research site, and a smaller developmental system which was housed in a separate trailer for mobility. The output

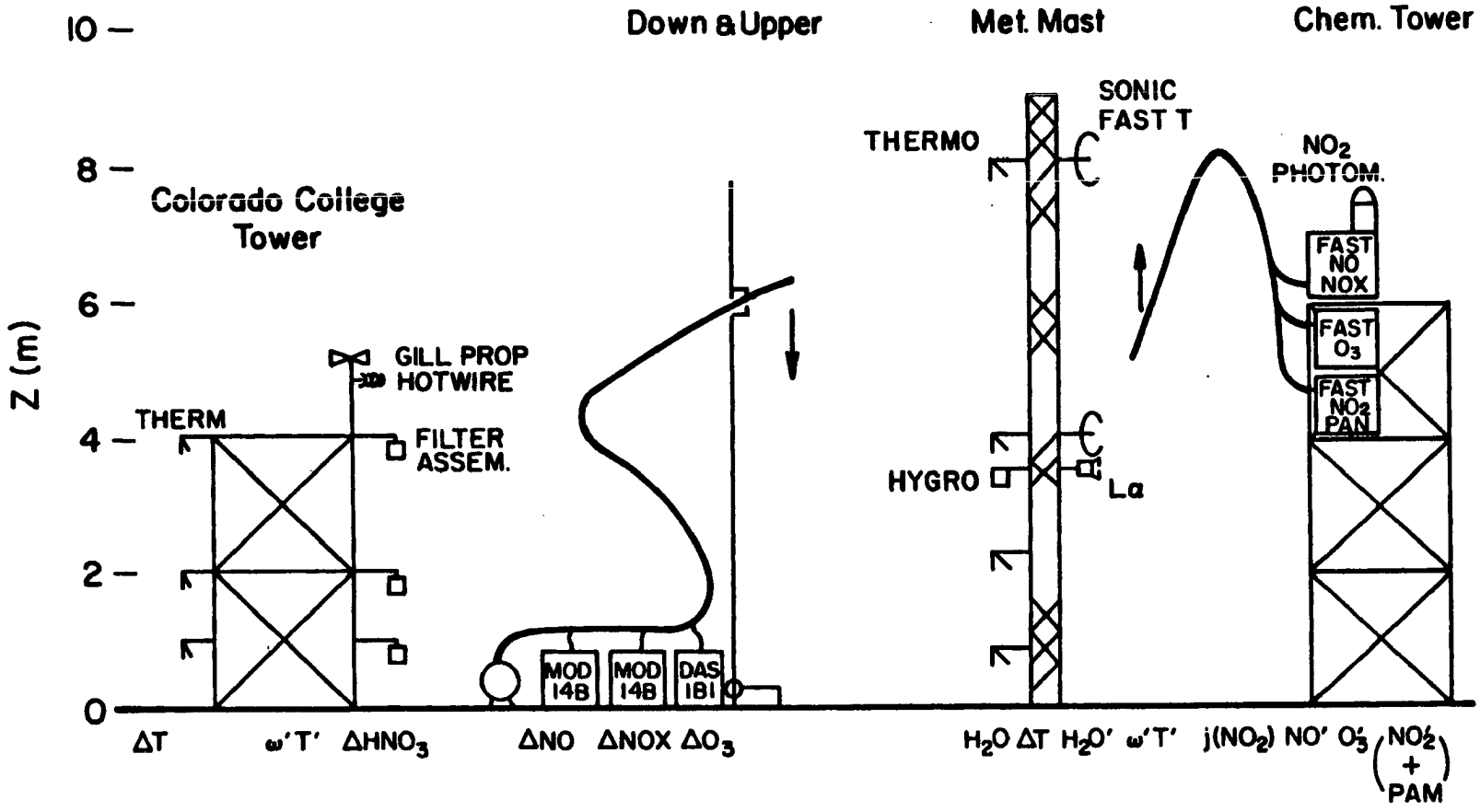

Figure 14. SLACE instrumentation and support structures [source: A. C. Delany]. The parameters measured are indicated below each tower. The "down and upper" is an automatic, motorized carriage that moves an aspirated sampling line between two measurement heights to obtain concentration gradients. The sample inlets of the three fast instruments could be positioned in turn near two sonic annemometers to detect evidence of vertical flux divergence.

of each instrument was connected in parallel to input channels on each data system. The BAO data system [Kaimal and Gaynor, 1983] is based on a PDP-11 computer capable of recording 16 channels at 10 Hz plus 16 channels at 1 Hz. Data summaries are output every 1.2 ks (20 min), and raw data are recorded on magnetic tape for up to 32 ks (9 hours) per tape. The developmental data acquisition system is based on a Zilog microcomputer capable of recording 10 channels at 10 Hz plus 22 channels at 1 Hz. Data were stored on floppy disks of 300-kilobyte capacity, which limited the possible continuous recording time to approximately 4.5 ks (75 min). Recording had to be interrupted when each disk was filled in order to transfer the data to magnetic tape. The data record from the developmental system, comprised as it is of discrete 4.5-ks segments, is much less convenient to work with than the 32-ks continuous records produced by the BAO system. For this reason data from the BAO system were used almost exclusively for the data analysis. The complete data record of the SLACE experiment comprises 30 volumes of magnetic tape, each carrying about 35 megabytes of data.

Flux Comparison Experiment

To find the fluxes of heat, O_3, NO and NO_2 by the eddy correlation method requires sensors for the vertical wind, temperature, and the three gas concentrations, each sampled at a rate of 10 Hz. Sonic anemometers were located at 4.66 m and 8.86 m (nominally 4 m and 8 m), each with a platinum wire thermometer near the center of its accoustic path. The fast chemical sensors were placed on a separate scaffold 2 meters away to isolate the sonic annemometers from the vibration of vacuum pumps associated with the chemical sensors. To assure that the

measurements of vertical velocity and gas concentration were made simultaneously in a small spatial region, as required by the eddy correlation technique, the inlets to the chemical sensors were run out on a boom to within inches of the sonic's accoustic path. The time lag for sample air to pass through the inlet lines to the sensors were measured so that in the data analysis the concentration time series could be made simultaneous with the vertical wind time series for the correlation computations. The time lags varied from fractions of a second for O_3 and NO to nearly 7 seconds for NO_2. The chemical sensors are each one-of-a-kind units designed to meet the speed and sensitivity requirements of the eddy correlation technique. The ozone instrument [Pearson and Stedman, 1980] is based on chemiluminescence with reagent NO, while the NO instrument, developed by A.C. Delany, is based on chemiluminescence with reagent ozone. The NO_2 instrument is based on the light-emitting reaction of NO_2 with a solution containing liquid luminol [Wendel et al., 1983].

To find the flux by the modified Bowen ratio method requires measurement of heat flux and the gradients of chemical concentration and temperature. The temperature gradient was obtained using a system marketed by Weathertronics, which produces a signal proportional to the difference in temperature between two levels. Four sensors were nominally located at 1, 2, 4, and 8 meters. The response time of these instruments is about 15 seconds, and they were sampled once per second.

The system for measuring the chemical gradients (the "down and upper") is shown schematically in Figure 14. The single aspirated sampling line supplies all three instruments. The gradient is obtained by raising and lowering the inlet of the sampling line, so that a

concentration is obtained at two levels alternately. The inlet line was moved automatically by a motorized carriage programmed to operate between 1 and 6 meters. The cycle time was 360 s: transitions occured every 180 s, with 18 s required for the inlet line to reach the new level.

Nitric oxide and NO_x were sampled using modified Thermo Electron Corporation Model 14B chemiluminescent NO_x detectors [Delany et al., 1982]. The modifications include a larger reaction chamber, a faster vacuum pump and a pre-reactor for instrument background determination, providing about a ten-fold improvement over the detection limit of an off-the-shelf unit. The ozone measurements were made with a conventional Dasibi ozone analyzer, Model 1008-AH.

An example of the output of the chemical gradient system is shown in Figure 15. This case occurred at night with light winds and a stable atmosphere that limited vertical mixing. Under these conditions the surface sink can produce quite a dramatic concentration gradient in the surface layer. In daytime, vertical mixing is greater, and the gradient is seldom so obvious in the time series.

Flux Comparison Data Processing

The sole application of the flux comparison data in this paper is contained in Figure 1, from which we conclude that significant sampling error is present in the measured ozone gradient. This section briefly summarizes the data processing that leads to comparisons like that of Figure 1. Data reduction for the flux comparison experiment included

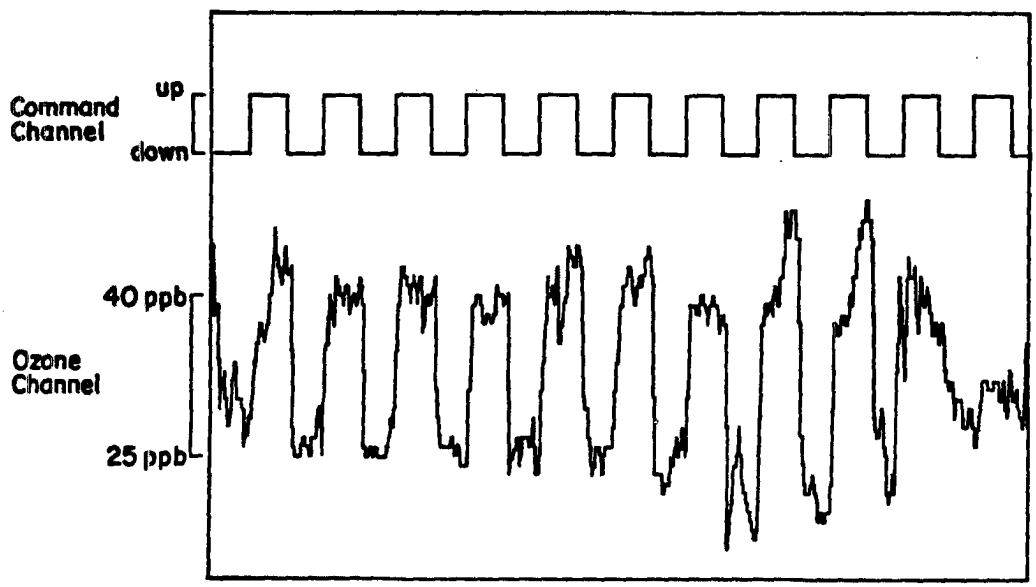

Figure 15. Example output from the concentration gradient system. The lower trace is ozone concentration from about 4 AM to 5 AM (MST), 7 July 1985, displaying the stair-step output characteristic of the Dasibi ozone monitor. The upper trace is the signal from the down and upper indicating its position. It is clear that the concentration is higher at 6 meters than at at 1 meter, consistent with the ideas of downward ozone flux and depletion at the surface. The gradient is calculated by averaging together a number of consecutive up and down periods, then taking the difference.

determining the fluxes of O_3, NO, and NO_2 by both the eddy correlation method

$$F_s = \overline{w's'}$$

(using 10-Hz data) and by the modified Bowen ratio method

$$F_s = \overline{w'T'}\ \Delta\bar{s}/\Delta\bar{\theta}$$

(using 1-Hz data). These tasks suggested a natural division of labor: the eddy correlation computations (including $\overline{w'T'}$) were performed by David Fitzjarrald at NCAR/MRS; and computation of the gradients $\Delta\bar{s}$ and $\Delta\bar{\theta}$ was carried out by the author at CSU. Computer resources for both efforts were provided by the Scientific Computing Division of NCAR.

Initial Editing

Each tape contained 38 megabytes of data, of which the 16 channels of 1 Hz data comprised only 3%. During the first pass through the data, the relevant data were extracted to form a smaller subset that would be simpler to work with. Raw data were in the form of 16-bit integers representing counts of the analog-to-digital converter. However, the integer format of PDP-11 machine that wrote the data tapes was not compatible with integer format of the CRAY machines on which the processing was carried out. Each integer was recorded on tape with the eight low-order bits first, followed by the eight high-order bits. Bit-manipulation utilities available on the CRAY were used to during the tape reading process to restructure the integer data in CRAY format.

Editing of NO and NO_x Data

The NO and NO_x channels required a special editing step for two reasons. First, the NO and NO_x instruments had been modified to increase their sensitivity, including provision for the instrument to

regularly switch into a background mode to establish the output for zero NO or NO_x. A separate data channel was used to record when each instrument was in the data or the background mode. Second, these instruments had front-panel range switches to keep the output voltage within a usable range over a wide range of gas concentrations. Because the range setting was changed by hand as gas concentration varied throughout the day, range changes were written in the log of the experiment and therefore had to be input to the data processing program by hand.

Two validity criteria were established for each data segment: it must be preceeded and followed by complete background segments; and there may be no range change in either background segment or the data segment. The first step was thus to read through the "mode" channels for the NO and NO_x instruments and list the beginning and end points of each background period. Using this listing and the experimental log, all range changes and incomplete background periods were identified, and a code number meaning "no data" was then substituted for each value in data segments not meeting the validity criteria. Since the background was continually changing with temperature throughout the day, a continuous background signal was generated between each pair of background periods using linear interpolation. The time-varying background value was subtracted from each value in each data segment and, finally, the resulting values were corrected for range by multiplying by the appropriate factor. The result of the editing process was a continuous series of 1-Hz NO or NO_x data with consistent scaling, interrupted by the "no data" code during each background period or any other period which had been rejected by the validity criteria.

Channel Summaries

The temperature, O_3, NO, and NO_x data were summarized by taking the mean over 180-s (3-min) periods corresponding to half-cycles of the down and upper. (Once in this form the data could be further averaged over longer times according to the various goals of SLACE.) The down and upper channel indicates at each second whether the "up" command or the "down" command is in effect. This channel was read to establish the time and direction of each transition command. For the four stationary temperature channels, an averaging period begins with each transition command of the down and upper and ends with the following transition command. For the three channels associated with the down and upper (chemical concentrations), 18 seconds of data were disregarded following each transition command, corresponding to the transit time of the down and upper, to assure that the data summaries would include only those values obtained either at 1 or 6 meters.

20-Minute Mean Gradients

The heat flux $\overline{w'T'}$ was provided for standard 1.2-ks (20-min) periods, which determined the averaging time for the gradients. First the start and stop times of the 1.2-ks (20-min) averaging periods and the 180-s (3-min) channel summaries were compared; only channel-summary periods that fell completely within the averaging periods were used to compute the mean gradient. For the three gas concentration channels, up periods and down periods were separately averaged, then subtracted. The four temperature channels were simply averaged. Finally, a channel-specific calibration factor was applied to obtain the 1.2ks (20-min) mean.

Because temperature sensors were not located at the upper and lower position of the down and upper, the temperature gradient was found by interpolation. For each period a regression equation of the form

$$\theta(z) = a + b \ln(z)$$

was fit to the mean temperature at 1, 2, 4, and 8 meters. Then the desired temperature gradient was computed by twice evaluating the regression equation, ie.,

$$\Delta\theta = \theta(6\ m) - \theta(1\ m)$$

APPENDIX B

TEMPERATURE GRADIENT DATA SET

The research in Chapters 2 and 3 is based upon temperature gradient measurements during the Surface Layer Atmospheric Chemistry Experiment (SLACE). This appendix describes the processing of this data into the form used in those chapters and summarizes the meteorological conditions during data collection.

Data Acquisition

The temperature sensors were the platinum-resistance-wire type, Model DT1A, manufactured by Atmospheric Instrumentation Research (AIR, Inc., 1880 South Flatiron Court, Boulder, Colorado 80301). Sensors were placed at 8.86 m and 4.66 m (nominally 8 m and 4 m). Signal conditioning circuits of the Model DT1A produce an output of 0.1 volt/°C with the same sign as the Celsius temperature (output range ±5 VDC, ±50 °C). A constant +5 volt offset was added to the temperature signal to match the signal range to the input voltage range of the data acquisition system (0-10 VDC). Following the offset step the signal was converted from voltage to frequency for transmission to the data acquisition system. There it was reconverted from frequency to voltage and input to an analog-to-digital converter. Each temperature channel was sampled at 10 Hz and the resulting integer data (counts of the A-D converter) were recorded on magnetic tape for up to nine hours, the limit imposed by tape capacity. The data acquisition system was

provided by the Boulder Atmospheric Observatory (BAO) and is described in detail by Kaimal and Gaynor [1983]. A very useful feature of the BAO data system is the standard data summary produced every 1.2 ks (20 min) giving the mean of each channel and several derived quantities; these summaries allow us to characterize the meteorological conditions during the SLACE field study.

Calibration

The integer data were converted to degrees Celsius using

$$°C = (\text{counts} \times .002 \text{ volts/count} \times 10°C/\text{volt}) - 50°C$$

where the subtraction removes the voltage offset introduced earlier. No calibration against an independent temperature standard was attemped in the field, and no further consideration was given to calibration of the signal path elements: absolute calibration of the sensors and signal path elements is not essential because of the way the temperature data are used in this study. The data are used two ways, to find the variance spectrum of temperature at the 8-m level, and to compare the temperature gradient calculated by two different methods (continuous and intermittent) from the same data. Computation of the spectrum is insensitive to absolute error in the data because the mean and linear trend are first removed from the time series; it is only required that the calibration does not vary over a 1.2-ks (20-min) run and this may be reasonably assumed. The comparison of the intermittent and continuous method for calculating the gradient is valid regardless of absolute error which may be present in the gradient measurements. The value of the intermittent sampling error (9) is sensitive to ΔT_c, which appears

in the denominator, but the only requirement is that the ΔT_C values should be reasonable for the atmospheric conditions of interest, which they are.

Data Processing

Initial preparation of the data set included interpolation of 1-Hz data, removal of the diurnal variations, and segmentation into half-hour cases, or "runs". The data were converted from 10 Hz to 1 Hz to be consistent with the typical sampling rate used in a scalar gradient measurement and to make maximum possible use of computer programs that had been previously developed for 1-Hz data. The 10 Hz time series were first filtered with a low-pass digital filter [Holloway, 1958] to avoid contamination of the 1 Hz time series with aliases of frequencies higher than the sampling rate [Blackman and Tukey, 1958]. The Nyquist, or folding, frequency is defined by $f_N=1/(2dt)$, where the sampling interval dt = 1 s. Filtering above this frequency was acomplished using a triangular filter with 17 weights. This filter has a response of 0.53 at 0.5 Hz, ie., it attentuates by a factor of 2 at the Nyquist frequency. Every 10th data point in the filtered 10-Hz time series was taken as a data point in the new 1-Hz time series.

The presence of a strong diurnal component in the temperature time series presents a problem in that the gradient computed by the intermittent method is affected by the presence of a linear trend. To avoid this problem, discussed in Chapter 3, the diurnal variation was removed from the temperature time series. A second-order polylnominal was fitted to the 8-m temperature time series from each 9-hour data tape using the method of least squares, and the resulting polynomial was subtracted from both the 4 m and 8 m temperature time series. The

procedure is illustrated in Figure 16 which shows the 1 Hz timeseries at 8 m before and after the removal of the second-order polynomial. This step removes the diurnal variations from both time series but leaves intact the variance contributed by wavelengths shorter than about 86 ks (24 hours), and does not alter the temperature-difference time series in any way. These steps produce two time series of about 32-ks (9-hour) length for each data tape.

The Data Set

The process described above was done for four tapes, covering the periods shown in Table 1. These tapes were selected for their high proportion of unstable atmospheric conditions, using negative 1.8-ks (30-min) mean temperature gradient as the acceptance criterion. As shown in Table 1 some data was discarded in the early morning prior to onset of unstable lapse rate in the surface layer. After editing, the four tapes comprise a data record of 76 ks (21 hours). The meteorological conditions during the periods covered by the data set are given in Table 2 as 1.2-ks (20-min) means at 10 m provided by the BAO data system.

TABLE 1.-- Data set coverage.

Tape name	Date	Time (MST)	Data set coverage (MST)
B05067	29 Jun 83	0840-1400	0840-1340
B03145	30 Jun 83	0800-1340	0830-1330
B03149	1 Jul 83	0540-1340	0640-1340
B03170	2 Jul 83	0700-1320	0900-1300

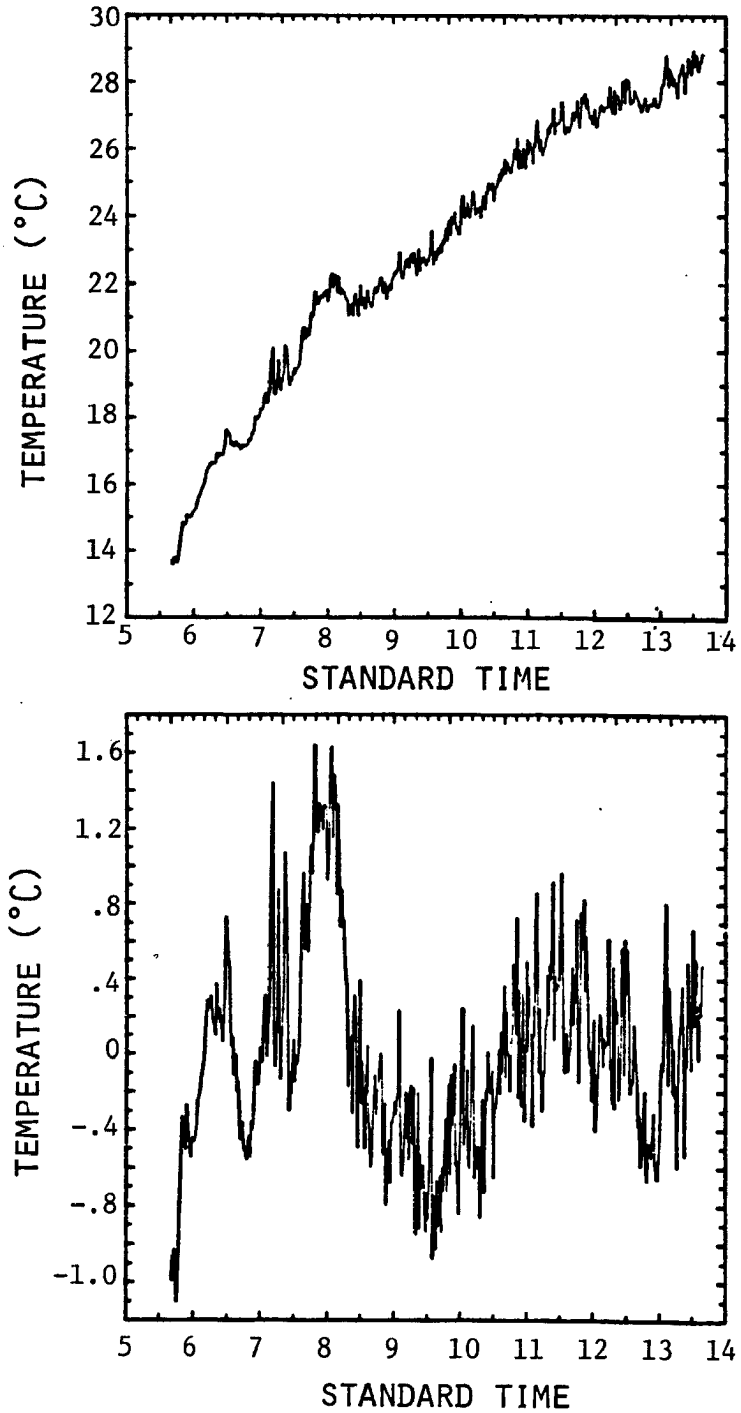

Figure 16. Removal of diurnal variation. A second-order polynomial is fit to the 60-s mean temperature at the 8-m level (upper frame). The lower frame shows the same time series after subtracting the polynomial. Data are from Tape B03149, 1 July 83.

TABLE 2.-- Meteorological data at z=10 m. Mean horizontal wind u (m/s), direction D (degrees), temperature T (°C), dew point Td (°C), and Obukhov length L (m) for 62 periods of length 1.2 ks (20 min), beginning at times shown (Mountain Standard Time).

MST	u	D	T	Td	L	MST	u	D	T	Td	L
	(29 Jun 85)						(1 Jul 85)				
0840	2.5	131	19	NA*	NA	0640	2.5	246	18	7	-26
0900	2.0	114	19	NA	NA	0700	1.4	258	19	7	-11
0920	2.3	126	20	NA	NA	0720	1.2	215	20	8	-19
0940	0.8	129	20	NA	NA	0740	0.6	133	22	8	-12
1000	1.1	169	20	NA	NA	0800	1.3	118	23	7	- 1
1020	1.8	182	21	NA	NA	0820	1.9	129	23	9	-17
1040	2.5	171	21	NA	NA	0840	2.7	122	23	9	-27
1100	2.9	159	22	NA	NA	0900	3.0	145	24	9	-13
1120	3.2	148	22	NA	NA	0920	3.8	143	24	9	-57
1140	2.9	154	23	NA	NA	0940	3.5	134	25	9	-45
1200	3.4	143	23	NA	NA	1000	3.0	136	26	9	-48
1220	2.7	143	23	NA	NA	1020	3.1	148	27	9	-40
1240	2.4	166	24	NA	NA	1040	3.3	131	27	10	-29
1300	2.3	141	24	NA	NA	1100	3.4	152	28	7	-42
1320	1.8	202	25	NA	NA	1120	3.4	162	29	3	-42
						1140	3.2	158	29	2	-27
	(30 JUN 85)					1200	3.1	159	29	4	-30
						1220	2.7	140	29	2	-32
0820	1.7	162	22	8	-35	1240	2.4	135	29	2	-45
0840	1.8	196	23	8	-20	1300	1.7	104	29	NA	-19
0900	2.0	194	25	9	-28	1320	2.0	106	30	NA	-26
0920	1.3	185	25	10	-20						
0940	1.3	199	26	10	-12		(2 Jul 85)				
1000	0.7	273	27	10	-27						
1020	1.2	86	28	8	- 4	0900	4.2	248	26	3	-79
1040	1.5	63	28	9	-20	0920	4.2	266	27	2	-55
1100	2.3	52	28	8	- 4	0940	4.8	284	28	1	-33
1120	2.2	63	28	5	-20	1000	5.7	286	28	0	-86
1140	3.2	65	28	4	-11	1020	4.6	274	28	0	-75
1200	3.5	63	29	4	-20	1040	4.4	287	28	-1	-21
1220	3.2	97	29	3	-29	1100	3.9	289	29	0	-21
1240	3.6	81	29	4	-54	1120	5.1	285	29	0	-73
1300	3.5	92	29	NA	-53	1140	3.9	272	29	0	- 7
1320	3.8	80	29	NA	-35	1200	2.9	258	29	0	-18
						1220	2.9	277	30	1	- 9
						1240	1.0	221	30	1	- 5

* not available

A subset of the data (Tape B03149) is used in Chapter 2 to evaluate the averaging time equation. The time series were subdivided into 1.2-ks (20-min) segments for computation of spectra. Table 3 gives the mean and variance of ΔT returned by the spectral analysis program (SPECFT).

Mean Wind Below 10 Meters

The estimation of generalized timescales for T and ΔT (Chapter 2) requires mean wind speed at 8.9 m and 6.4 m, but the lowest wind sensors were at 10 m, on the BAO tower. Winds below 10 m were estimated using the diabatic wind profile in its integrated form [Panofsky and Dutton, 1984]

$$u(z) = (u_*/k_a)\,[\ln(z/z_o) - \psi(z/L)]$$

$$\psi = \ln\{\,[(1+x^2)/2]\,[(1+x)/2]^2\,\} - 2\tan^{-1}x + (\pi/2)$$

$$x = [1 - 16(z/L)]^{1/4}$$

where u_* is the friction velocity, k_a the Von Karman constant, L the Obukhov length, z_o the roughness length [$\bar{u}(z_o)=0$], and x is the well-known Businger-Dyer form of the diabatic wind profile. If we form the ratio $\bar{u}(z)/\bar{u}(z_1)$ where z_1=10 m, then

$$\bar{u}(z) = \bar{u}(z_1)\,\{\,[\ln(z/z_o)-\psi(z/L)]\,/\,[\ln(z_1/z_o)-\psi(z_1/L]\,\} \qquad (16)$$

This expression gives an estimate of the mean wind at height z given the 10-m wind speed, z_o, and L. The roughness length is estimated to be 0.05 m, based on the average vegetation height 0.8 m. The Obukhov length is calculated by the BAO data system from the heat flux and momentum flux at the 10-m level; 1.2-ks (20-min) mean values of L are given in Table 2. Equation (16) was evaluated for the 21-case data subset, with the result that average wind speed is 2.5 m s^{-1} at 8.9 m, and 2.4 ms^{-1} at 6.4 m (the geometric mean measurement height.)

TABLE 3.-- Mean and variance of ΔT for tape B03149, 1 Jul 85. Periods begin at time shown (Mountain Standard Time).

MST	$\overline{\Delta T}$	$\overline{(\Delta T)'^2}$	$\overline{(\Delta T)'^2}/\overline{\Delta T}^2$
0640	-0.23	0.03	0.50
0700	-0.37	0.13	0.97
0720	-0.39	0.19	1.22
0740	-0.36	0.11	0.85
0800	-0.43	0.17	0.92
0820	-0.44	0.11	0.59
0840	-0.51	0.07	0.27
0900	-0.53	0.12	0.44
0920	-0.56	0.08	0.26
0940	-0.61	0.10	0.25
1000	-0.63	0.11	0.28
1020	-0.64	0.14	0.35
1040	-0.78	0.16	0.25
1100	-0.73	0.12	0.22
1120	-0.77	0.15	0.26
1140	-0.69	0.11	0.26
1200	-0.71	0.11	0.22
1220	-0.75	0.12	0.21
1240	-0.59	0.02	0.07
1300	-0.74	0.12	0.22
1320	-0.83	0.16	0.23

APPENDIX C

DERIVATION OF THE DEADTIME EQUATION

The response $E_o(t)$ of a gas monitoring instrument to a step change in concentration $E_i(t)$ may usually be characterized as exponential decay. The instrument reponse time t_r is the time required for the displacement $E_o - E_i$ to be reduced to 1/e times its initial value (the e-folding time). For such an instrument E_o and E_i are related [Kaplan, 1981] by

$$(dE_o/dt) + (E_o/t_r) = (E_i/t_r) \tag{17}$$

We shall now suppose that gas concentration changes according to the ramp function of Figure 10 so that

$$\begin{aligned} E_i &= (E_1/t_e)t, \quad 0 < t < t_e \\ E_i &= E_1 \quad , \quad t_e \leq t \end{aligned} \tag{18}$$

General solutions to (17) are given by Kaplan [1981] for both portions of this forcing function. For the ramp portion of (18) the solution is

$$E_o = (E_1 t_r/t_e) \left[(t/t_r) - 1 + \exp(t/t_r) \right] + C \exp(-t/t_r) \tag{19}$$

We may use the boundary condition that $E_o=0$ at $t=0$ to evaluate the constant C; substitution into (19) gives the result $C=0$ so that the solution for the ramp portion of the forcing function becomes

$$E_o = (E_1 t_r/t_e) \left[(t/t_r) - 1 + \exp(t/t_r) \right] \tag{20}$$

For times $t \geq t_e$ the forcing function is constant. The general solution to (17) for constant forcing is

$$E_o = E_1 \left[1 - \exp(-t/t_r) \right] + D \exp(-t/t_r) \tag{21}$$

Now we may evaluate the constant D by matching these two solutions at $t=t_e$ (at the upper end of the ramp). Then we have

$$(E_1 t_r/t_e)[(t/t_r)-1+\exp(t/t_r)]=E_1[1-\exp(-t/t_r)]+D\exp(-t/t_r)$$

which, after some manipulation, reduces to

$$D = E_1 \left[(t_r/t_e) - (t_r/t_e) \exp(t_e/t_r) + 1 \right] \tag{22}$$

Substituting (22) into (21) we obtain the final solution

$$E_o = E_1[1-\exp(-t/t_r)] + E_1[(t_r/t_e)-(t_r/t_e)\exp(t_e/t_r)+1] \exp(-t/t_r)$$

which reduces to the form given in Chapter 3,

$$\begin{aligned} E_o/E_1 &= 1 - A \exp(-t/t_r) \\ A &= (t_r/t_e) \left[\exp(t_e/t_r) - 1\right] \end{aligned} \tag{12}$$